Buildup and transient oscillations of Andreev quasiparticles

R. Taranko and T. Domański*
Institute of Physics, M. Curie Skłodowska University, 20-031 Lublin, Poland

(Received 31 May 2017; revised manuscript received 25 May 2018; published 21 August 2018)

We study transient effects in a setup where the quantum dot is abruptly sandwiched between the metallic and superconducting leads. Focusing on the proximity-induced electron pairing manifested by the in-gap bound states, we determine characteristic timescales needed for these quasiparticles to develop. In particular, we derive analytic expressions for (i) charge occupancy of the quantum dot, (ii) amplitude of the induced electron pairing, and (iii) the transient currents under equilibrium and nonequilibrium conditions. We also investigate the correlation effects within the Hartree-Fock-Bogolubov approximation, revealing a competition between the Coulomb interactions and electron pairing.

DOI: 10.1103/PhysRevB.98.075420

I. INTRODUCTION

Quantum impurity hybridized with any superconducting bulk material is influenced by the Cooper pairs which leak into its region, developing the quasiparticle states in the subgap spectrum $|\omega| \leqslant \Delta$ (where Δ is the energy gap of superconducting reservoir) [1,2]. These Andreev (or Yu-Shiba-Rusinov) states have been observed in numerous scanning tunneling microscopy studies, using impurities deposited on superconducting substrates [3,4] and in tunneling experiments via quantum dots (QDs) arranged in the Josephson [5], Andreev [6], and more complex (multiterminal) configurations [7,8]. Since measurements can be nowadays done with state-of-the-art precision probing the time-resolved properties, we address this issue here and determine some characteristic temporal scales of the in-gap quasiparticles.

Any abrupt change of the model parameters (*quantum quench*) is usually followed by a time-dependent thermalization of the many-body system, where continuum states play a prominent role [9]. Dynamics of these processes has been recently explored in the solid state and nanoscopic physics [10]. From a practical point of view, especially useful could be nanoscopic heterostructures with the correlated QD embedded between external (metallic, ferromagnetic, or superconducting) leads, which enables measurements of the transport properties under tunable nonequilibrium conditions [11].

Transport phenomena through QD coupled between the normal or superconducting leads have been so far explored predominantly in the static cases. Since new experimental methods allow us to study the QDs subjected to voltage pulses or abrupt changes of the system parameters, it would be very desirable to calculate the time-dependent currents and their conductances. In particular, one can ask the question: *How fast does the QD respond to an instantaneous perturbation*? For this purpose, analytical estimation of the transient oscillations and long-time (asymptotic) behavior of the measurable quantities would be very useful. Some early theoretical works have investigated time-dependent transport via QD between the normal and superconducting leads [12–15], however, analytic results are hardly available. As regards the QD coupled to both normal leads, the transient current and charge occupancy have been determined for abrupt voltage pulses or after an instantaneous switching of constituent parts of the system [16–32].

Time-resolved techniques could provide an insight into the many-body effects. For instance, the pump-and-probe experiments [33] and the time-resolved angle resolved photoemission spectroscopy [34] have determined the lifetime of the Bogoliubov quasiparticles in the high-temperature superconductors. Transient effects have been investigated in nanoscopic systems, considering mainly the QDs hybridized with the conducting (metallic) leads. There has been studied the timescale needed for the Kondo peak to develop at the Fermi energy [35], dynamical correlations in electronic transport via the QDs [36], or oscillatory behavior in the charge transport through the molecular junctions [37].

Dynamical phenomena of the QDs attached to superconducting bulk reservoirs have been studied much less intensively. There have been analyzed: photon-assisted Andreev tunneling [38], response time on a steplike pulse [39], temporal dependence of the multiple Andreev reflections [40], time-dependent sequential tunneling [41], transient effects caused by an oscillating level [42], time-dependent bias [43], waiting time distributions in nonequilibrium transport [44–47], short-time counting statistics [48–50], metastable configurations of the Andreev bound states in a phase-biased Josephson junction [9,51], finite-frequency noise [52], superconducting proximity effect in interacting QD, and double-dot systems [53,54]. None of these studies, however, addressed the timescale typical for development of the subgap quasiparticle states in a setup, comprising the QD coupled to the normal lead (N) on one side and to the isotropic (s-wave) superconductor (S) on the other side. Our present study reveals that a continuous electronic spectrum of the metallic lead enables a relaxation of the Andreev states, whereas the superconducting electrode induces the (damped) quantum oscillations with a period

*doman@kft.umcs.lublin.pl

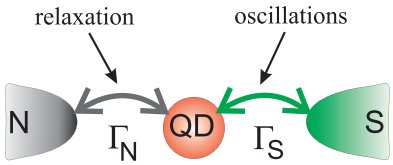

FIG. 1. Schematics of the setup, comprising the quantum dot (QD) coupled to the normal (N) and superconducting (S) electrodes. Sudden coupling to the continuum states triggers the relaxation processes, whereas the superconductor induces the in-gap bound states, giving rise to quantum oscillations.

sensitive to the energies of the in-gap quasiparticles. In what follows, we evaluate the timescale at which such Andreev quasiparticle start to form, and another when they are finally established.

The paper is organized as follows. In Sec. II, we introduce the microscopic model and discuss the method for the time-dependent phenomena. Section III presents analytical results for the uncorrelated QD, such as (i) charge occupancy, (ii) complex order parameter, and (iii) charge current for the unbiased and biased heterojunction. In Sec. IV, we discuss the correlation effects and, finally, in Sec. V we summarize the main results.

II. MICROSCOPIC MODEL

For a description of the N-QD-S heterostructure (see Fig. 1), we use the single impurity Anderson Hamiltonian

$$\hat{H} = \sum_{\sigma} \varepsilon_{\sigma} \hat{d}_{\sigma}^{\dagger} \hat{d}_{\sigma} + U\, \hat{n}_{\uparrow} \hat{n}_{\downarrow} + \sum_{\beta} (\hat{H}_{\beta} + \hat{V}_{\beta-\mathrm{QD}}), \qquad (1)$$

where β refers to the normal (N) and superconducting (S) electrodes, respectively. As usual, $\hat{d}_{\sigma}$ ($\hat{d}_{\sigma}^{\dagger}$) is the annihilation (creation) operator for the QD electron with spin σ and energy ε_{σ}. Potential of the Coulomb repulsion between the opposite spin electrons is denoted by U. We treat the external metallic lead as free fermion gas $\hat{H}_N = \sum_{\mathbf{k},\sigma} \varepsilon_{\mathbf{k}} \hat{c}_{\mathbf{k}\sigma}^{\dagger} \hat{c}_{\mathbf{k}\sigma}$, and describe the isotropic superconductor by the BCS model $\hat{H}_S = \sum_{\mathbf{q},\sigma} \varepsilon_{\mathbf{q}} \hat{c}_{\mathbf{q}\sigma}^{\dagger} \hat{c}_{\mathbf{q}\sigma} - \sum_{\mathbf{q}} \Delta(\hat{c}_{\mathbf{q}\uparrow}^{\dagger} \hat{c}_{-\mathbf{q}\downarrow}^{\dagger} + \hat{c}_{-\mathbf{q}\downarrow} \hat{c}_{\mathbf{q}\uparrow})$, where $\varepsilon_{\mathbf{k}(\mathbf{q})}$ is the energy measured from the chemical potential $\mu_{N(S)}$, and Δ denotes the superconducting energy gap. Hybridization between the QD electrons and the metallic lead is given by $\hat{V}_{N-\mathrm{QD}} = \sum_{\mathbf{k},\sigma} (V_{\mathbf{k}}\, \hat{d}_{\sigma}^{\dagger} \hat{c}_{\mathbf{k}\sigma} + \mathrm{H.c.})$ and $\hat{V}_{S-\mathrm{QD}}$ can be expressed by interchanging $\mathbf{k} \leftrightarrow \mathbf{q}$.

Since our study refers to the subgap quasiparticle states, we assume the constant couplings $\Gamma_{N(S)} = 2\pi \sum_{\mathbf{k}(\mathbf{q})} |V_{\mathbf{k}(\mathbf{q})}|^2\, \delta(\omega - \varepsilon_{\mathbf{k}(\mathbf{q})})$. In the deep subgap regime $|\omega| \ll \Delta$ (the so-called superconducting atomic limit), the coupling $\Gamma_S/2$ can be regarded as a qualitative measure of the induced pairing potential, whereas Γ_N controls the inverse lifetime of the in-gap quasiparticles. As we shall see, both these couplings play important (though quite different) roles in transient phenomena.

We assume that all three constituents of the N-QD-S heterostructure are disconnected from each other until $t \leqslant 0$. Let us impose the external (N, S) reservoirs to be suddenly coupled to the quantum dot

$$V_{\mathbf{k}(\mathbf{q})}(t) = \begin{cases} 0 & \text{for } t \leqslant 0, \\ V_{\mathbf{k}(\mathbf{q})} & \text{for } t > 0, \end{cases} \qquad (2)$$

inducing the transient effects. Later on, we shall relax this assumption. Our problem resembles the Wiener-Hopf method [55] applied earlier in the studies of x-ray absorption and emission of metals [56].

In what follows, we explore the time-dependence of physical observables $\hat{O}$, based on the Heisenberg equation of motion $i\hbar \frac{d}{dt} \hat{O} = [\hat{O}, \hat{H}]$. In particular, we shall investigate expectation values of the QD occupancy $\langle \hat{d}_{\sigma}^{\dagger}(t) \hat{d}_{\sigma}(t) \rangle$, the induced on-dot pairing $\langle \hat{d}_{\downarrow}(t) \hat{d}_{\uparrow}(t) \rangle$, and the transient charge currents flowing between the QD and external electrodes (both under equilibrium and nonequilibrium conditions).

Our strategy is based on the following three steps: First, we formulate the differential equations of motion for the annihilation $\hat{d}_{\sigma}(t)$ and creation $\hat{d}_{\sigma}^{\dagger}(t)$ operators of QD and similar ones for the mobile electrons $\hat{c}_{\mathbf{k}(\mathbf{q})\sigma}(t)$ and $\hat{c}_{\mathbf{k}(\mathbf{q})\sigma}^{(\dagger)}(t)$, respectively. Next, we solve them using the Laplace transformations, e.g., for $\hat{d}_{\sigma}(t)$ we denote

$$\hat{d}_{\sigma}(s) = \int_0^{\infty} e^{-st} \hat{d}_{\sigma}(t) dt \equiv \mathcal{L}\{\hat{d}_{\sigma}(t)\}(s). \qquad (3)$$

For the uncorrelated QD, the analytical expressions for $\hat{d}_{\sigma}(s)$ and $\hat{d}_{\sigma}^{\dagger}(s)$ can be obtained (see Appendix A). Finally, using the corresponding inverse Laplace transforms, we compute the time-dependent expectation values of the QD occupancy, the QD pair amplitude, and currents flowing between QD and both leads. For example, QD occupancy $n_{\sigma}(t) \equiv \langle \hat{d}_{\sigma}^{\dagger}(t) \hat{d}_{\sigma}(t) \rangle$ is given by

$$n_{\sigma}(t) = \langle \mathcal{L}^{-1}\{\hat{d}_{\sigma}^{\dagger}(s)\}(t)\; \mathcal{L}^{-1}\{\hat{d}_{\sigma}(s)\}(t) \rangle, \qquad (4)$$

where $\mathcal{L}^{-1}\{\hat{d}_{\sigma}(s)\}(t)$ stands for the inverse Laplace transform of $\hat{d}_{\sigma}(s)$.

In our calculations, we make use of the wide-band-limit approximation ($\Gamma_{\beta} = \mathrm{const}$) and set $e = \hbar = k_B \equiv 1$, so that all energies, currents, and time are expressed in units of Γ_S, $e\Gamma_S/\hbar$, and $\hbar/\Gamma_S$, respectively. We also treat the chemical potential $\mu_S = 0$ as a convenient reference energy point and perform the calculations for zero temperature. For experimentally available value $\Gamma_S \sim 200\,\mu\mathrm{eV}$ [57–59], the typical times and current units would be ~3.3 psec and ~48 nA, respectively.

III. UNCORRELATED QD CASE

We start by addressing the transient effects of the uncorrelated quantum dot ($U = 0$), focusing on the superconducting atomic limit ($\Delta = \infty$) for which analytical expressions can be obtained. More general considerations are presented in Appendix A.

A. Time-dependent QD charge

Let us inspect the time-dependent occupancy $n_{\sigma}(t)$ driven by an abrupt coupling of the QD to both external leads. This quantity, defined in Eq. (4), can be determined explicitly for arbitrary Δ (derivation is presented in Appendix A). Here we shall consider the formula Eq. (A12) simplified for

the superconducting atomic limit:

$$n_\uparrow(t) = e^{-\Gamma_N t}\left\{ n_\uparrow(0) + [1 - n_\uparrow(0) - n_\downarrow(0)]\,\sin^2\left(\frac{\sqrt{\delta}}{2}\,t\right)\frac{\Gamma_S^2}{\delta}\right\}$$
$$+ \frac{\Gamma_N}{2\pi}\int_{-\infty}^{\infty} d\omega\;\; f_N(\omega)\;\mathcal{L}^{-1}\left\{\frac{s + i\varepsilon_{-\sigma} + \Gamma_N/2}{(s-s_1)(s-s_2)(s-i\omega)}\right\}(t)\;\;\mathcal{L}^{-1}\left\{\frac{s - i\varepsilon_{-\sigma} + \Gamma_N/2}{(s-s_3)(s-s_4)(s+i\omega)}\right\}(t)$$
$$+ \left(\frac{\Gamma_S}{2}\right)^2\frac{\Gamma_N}{2\pi}\int_{-\infty}^{\infty} d\omega\;\; [1 - f_N(\omega)]\;\mathcal{L}^{-1}\left\{\frac{1}{(s-s_1)(s-s_2)(s+i\omega)}\right\}(t)\;\;\mathcal{L}^{-1}\left\{\frac{1}{(s-s_3)(s-s_4)(s-i\omega)}\right\}(t), \quad (5)$$

where $f_N(\omega)$ is the Fermi-Dirac distribution function of the normal lead and we defined auxiliary parameters

$$s_{1,2} = \frac{i}{2}[(\varepsilon_\uparrow - \varepsilon_\downarrow) + i\Gamma_N \pm \sqrt{\delta}], \quad (6)$$

$$s_{3,4} = \frac{i}{2}[-(\varepsilon_\uparrow - \varepsilon_\downarrow) + i\Gamma_N \pm \sqrt{\delta}],\;\; s_34, \quad (7)$$

$$\delta = (\varepsilon_\uparrow + \varepsilon_\downarrow)^2 + \Gamma_S^2. \quad (8)$$

The occupancy $n_\downarrow(t)$ can be obtained from the same expression Eq. (5) upon replacing the set (s_1, s_2, s_3, s_4) by (s_3, s_4, s_1, s_2). Expressions given in the second and third lines of Eq. (5) could be presented in a more compact analytical form in the case $\varepsilon_\sigma = 0$ [see Eqs. (A14)–(A16)]. In the general case, they are rather lengthy (even though accessible), therefore we skip them.

Another simplification of Eq. (5) is possible upon neglecting the normal lead ($\Gamma_N = 0$). QD occupancy is then characterized by nonvanishing quantum oscillations:

$$n_\sigma(t) = n_\sigma(0) + [1 - n_\sigma(0) - n_{-\sigma}(0)]\,\sin^2\left(\frac{\sqrt{\delta}}{2}\,t\right)\frac{\Gamma_S^2}{\delta}. \quad (9)$$

For $\varepsilon_\sigma = 0$, Eq. (9) reduces to

$$n_\sigma(t) = \cos^2\left(\frac{\Gamma_S}{2}\,t\right)n_\sigma(0) + \sin^2\left(\frac{\Gamma_S}{2}\,t\right)[1 - n_{-\sigma}(0)], \quad (10)$$

implying the period of transient oscillations $T = 2\pi/\Gamma_S$, except of the initial conditions $n_\sigma(0) = 1$ and $n_{-\sigma}(0) = 0$ when the QD occupancy is preserved.

The formula Eq. (10), obtained in the case $\Gamma_N = 0$, resembles the Rabi oscillations of a typical two-level quantum system. Indeed, the proximitized QD is fully equivalent to such scenario. To prove it, let us consider the effective Hamiltonian $\hat{H} = \sum_\sigma \varepsilon_\sigma \hat{n}_\sigma + \frac{\Gamma_S}{2}(\hat{d}_\uparrow^\dagger \hat{d}_\downarrow^\dagger + \text{H.c.})$, assuming that at $t = 0$ the QD is empty $n_\uparrow(0) = 0 = n_\downarrow(0)$. For arbitrary time $t > 0$, we can calculate the probability $P(t)$ of finding the QD in the doubly occupied configuration $n_\uparrow(t) = 1 = n_\downarrow(t)$ within the standard treatment of a two-level system [60]. This probability is given by

$$P(t) = \frac{\Gamma_S^2}{(E_1 - E_2)^2 + \Gamma_S^2}\sin^2\left(\frac{t}{2}\sqrt{(E_1 - E_2)^2 + \Gamma_S^2}\right), \quad (11)$$

where $E_1 = 0$ and $E_2 = \varepsilon_\uparrow + \varepsilon_\downarrow$ are the energies of empty and doubly occupied configurations, respectively. This result exactly reproduces our expression Eq. (10).

For the QD suddenly coupled to both the normal and superconducting leads ($\Gamma_{N,S} \neq 0$), such oscillations become damped (see Fig. 2). This effect comes partly from the exponential factor $\exp(-\Gamma_N t)$ appearing in front of the first term in Eq. (5) and partly from the second and third contributions. This can be illustrated by considering the case $\varepsilon_\sigma = 0$, $\mu_N = 0$, for which Eq. (5) implies

$$n_\sigma(t) = e^{-\Gamma_N t}\left\{\cos^2\left(\frac{\Gamma_S}{2}t\right)n_\sigma(0) + \sin^2\left(\frac{\Gamma_S}{2}t\right)[1 - n_{-\sigma}(0)]\right\} + \frac{1}{2}(1 - e^{-\Gamma_N t}). \quad (12)$$

Under such circumstances, the QD occupancy approaches asymptotically a half-filling, $\lim_{t\to\infty} n_\sigma(t) = \frac{1}{2}$. Figure 2 displays $n_\uparrow(t)$ obtained in absence of external voltage for several values of Γ_N, assuming $\varepsilon_\sigma = 0$ and $n_\sigma(0) = 0$ for both spins. The quantum oscillations occur with a period $2\pi/\Gamma_S$ and their damping is governed by the envelope function $e^{-\Gamma_N t}$ indicating that a continuous spectrum of the metallic lead is responsible for the relaxation processes. For a weak enough coupling Γ_N, these oscillations could indirectly probe the dynamical transitions between the subgap bound states, as recently emphasized by J. Gramich *et al.* [8].

Figure 3 shows the QD occupancies obtained for several initial conditions, assuming $\mu_N = \mu_S = 0$ and $\varepsilon_\sigma = 0$. The case $n_\downarrow(0) = 0 = n_\uparrow(0)$ allows quantum oscillations between two eigenstates of the proximitized QD, which are damped due to

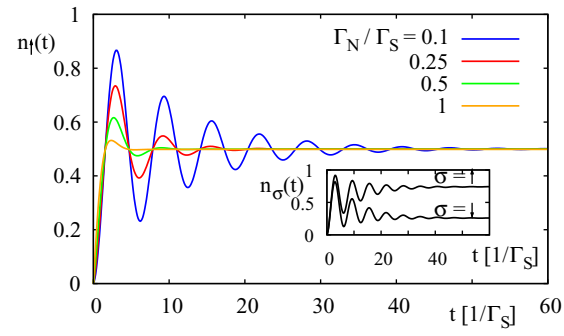

FIG. 2. Time-dependent occupancy $n_\uparrow(t) = n_\downarrow(t)$ obtained for $\varepsilon_\sigma = 0$, assuming the initial occupancy $n_\uparrow(0) = 0 = n_\downarrow(0)$ in absence of external voltage ($\mu_N = \mu_S = 0$). Different lines correspond to various ratios Γ_N/Γ_S, indicated in the legend. Inset shows the QD occupancies $n_\sigma(t)$ for the finite Zeeman splitting $\varepsilon_\downarrow - \varepsilon_\uparrow = \Gamma_S$, assuming $\Gamma_N/\Gamma_S = 0.1$.

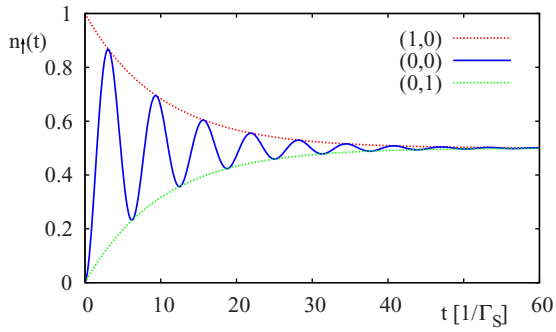

FIG. 3. The time-dependent QD occupancy $n_\uparrow(t)$ obtained in absence of external voltage for $\varepsilon_\sigma = 0$, $\Gamma_N = 0.1\Gamma_S$. Different curves refer to various initial occupancies $(n_\uparrow(0), n_\downarrow(0))$ indicated in the legend.

coupling to the normal lead (see Fig. 2). For the initial condition $n_\sigma(0) = 1$, $n_{-\sigma}(0) = 0$, the transient effects are completely different. The first term in Eq. (12) for $(n_\uparrow(0), n_\downarrow(0)) = (1, 0)$ or (0,1) equals $e^{-\Gamma_N t}$ or vanishes and together with the last term they yield $\frac{1}{2}(1 - e^{-\Gamma_N t})$—see the upper curve in Fig. 3 or $\frac{1}{2}(1 + e^{-\Gamma_N t})$—the lower curve, respectively. This stems from the fact that proximity-induced pairing affects only the empty and doubly occupied configurations and it is inefficient in the case considered here. In consequence, the quantum oscillations are absent and the QD occupancy exponentially evolves towards a half-filling. Let us also remark that for $\Gamma_S = 0$, Eq. (5) simplifies to the standard formula obtained by the nonequilibrium Green's function method [61] [see Eq. (A17)].

B. Development of the proximity effect

Occupancy of the QD only indirectly tells us about emergence of the subgap bound states. To get some insight into the superconducting proximity effect, we shall study here the time evolution of the order parameter $\chi(t) = \langle \hat{d}_\downarrow(t)\hat{d}_\uparrow(t)\rangle$. The general formula is explicitly given by Eq. (A21). Expressing its first two terms (which depend on the initial QD occupancy) the pair correlation function can be written as

$$\chi(t) = \left[(\varepsilon_\uparrow + \varepsilon_\downarrow)\left(1 - \cos\left(\sqrt{\delta}\, t\right)\right) + i\sqrt{\delta}\sin\left(\sqrt{\delta}\, t\right)\right] e^{-\Gamma_N t}\Gamma_S \frac{(n_\uparrow(0) + n_\downarrow(0) - 1)}{2\delta} - i\frac{\Gamma_N\Gamma_S}{4\pi}\Phi_\uparrow^*, \tag{13}$$

where

$$\Phi_\sigma = -\int_{-\infty}^{\infty} d\varepsilon f_N(\varepsilon)\mathcal{L}^{-1}\left\{\frac{s + i\varepsilon_{-\sigma} + \frac{\Gamma_N}{2}}{(s - s_1)(s - s_2)(s - i\varepsilon)}\right\}(t)\mathcal{L}^{-1}\left\{\frac{1}{(s - s_3)(s - s_4)(s + i\varepsilon)}\right\}(t)$$
$$+ \int_{-\infty}^{\infty} d\varepsilon[1 - f_N(\varepsilon)]\mathcal{L}^{-1}\left\{\frac{1}{(s - s_1)(s - s_2)(s + i\varepsilon)}\right\}(t)\mathcal{L}^{-1}\left\{\frac{s + i\varepsilon_\sigma + \frac{\Gamma_N}{2}}{(s - s_3)(s - s_4)(s - i\varepsilon)}\right\}(t). \tag{14}$$

In Appendix A, we show that for $\mu_N = 0$, the real part of $\Phi_\uparrow$ vanishes. Let us next analyze Eq. (13) for different initial conditions and values of the QD energy levels. For $n_\sigma(0) = 0$, $n_{-\sigma}(0) = 1$ and $\mu_N = 0$ the function $\langle \hat{d}_\downarrow(t)\hat{d}_\uparrow(t)\rangle$ is real and nonoscillating in time and is equal to $-\frac{\Gamma_N\Gamma_S}{4\pi}\mathrm{Im}\Phi_\uparrow$, regardless of ε_σ. However, for $\mu_N \neq 0$, also the imaginary part of $\langle \hat{d}_\downarrow(t)\hat{d}_\uparrow(t)\rangle$ equals $-\frac{\Gamma_N\Gamma_S}{4\pi}\mathrm{Re}\Phi_\uparrow$ and is nonoscillating function. For the initial conditions $(n_\sigma(0), n_{-\sigma}(0)) = (0, 0)$ or (1,1), the picture is completely different. Depending on the value of $\varepsilon_\uparrow + \varepsilon_\downarrow$, the real part of $\langle \hat{d}_\downarrow(t)\hat{d}_\uparrow(t)\rangle$ oscillates for $\varepsilon_\uparrow + \varepsilon_\downarrow = 0$ or is a smooth function of time for $\varepsilon_\uparrow + \varepsilon_\downarrow \neq 0$. Simultaneously, the imaginary part of the QD on-dot pairing oscillates irrespective of ε_σ. The oscillatory parts of $\langle \hat{d}_\downarrow(t)\hat{d}_\uparrow(t)\rangle$ are dumped via $e^{-\Gamma_N t}$ factor, emphasizing the crucial role of continuum states of the normal electrode in relaxation processes.

In Fig. 4, we show the imaginary part of the on-dot pairing $\langle \hat{d}_\downarrow(t)\hat{d}_\uparrow(t)\rangle$, assuming the initial QD occupancy $n_\sigma(0) = 0$. Period T of the damped quantum oscillations depends on the excitation energy between the subgap Andreev quasiparticles [8] via $T = 2\pi/\sqrt{(\varepsilon_\downarrow + \varepsilon_\uparrow)^2 + \Gamma_S^2}$. For $\mu_N = 0$, these oscillations are related to the transient current $j_{S\sigma}(t)$ flowing between the proximitized QD and the superconducting lead (see Sec. III C) in analogy to the Josephson junction comprising two superconducting pieces, differing in phase of the order parameter. On the other hand, the real part (Fig. 5) evolves monotonously to its asymptotic value, except of one particular case $\Gamma_N = 0$, when the real part of $\langle \hat{d}_\downarrow(t)\hat{d}_\uparrow(t)\rangle$ vanishes.

C. Transient currents for unbiased system

So far, we have discussed the quantities which are important, but unfortunately they are not directly accessible experimentally. Let us now consider the measurable currents $j_{N\sigma}(t)$ and $j_{S\sigma}(t)$, flowing from the QD to the external leads. Formally, the

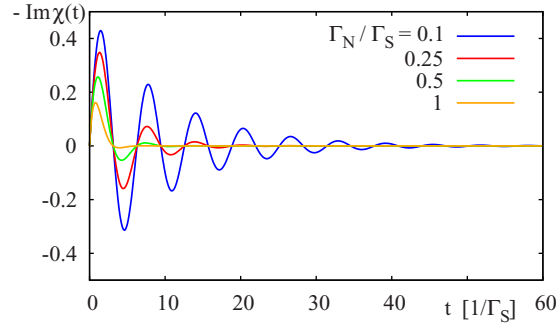

FIG. 4. The imaginary part of the induced on-dot pairing $\langle \hat{d}_\downarrow(t)\hat{d}_\uparrow(t)\rangle$ obtained for the same parameters as in Fig. 2.

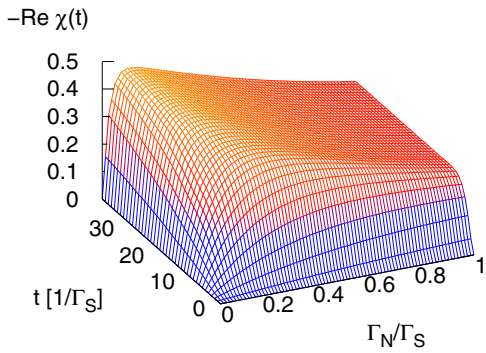

FIG. 5. The time-dependent real part of $\langle \hat{d}_\downarrow(t)\hat{d}_\uparrow(t)\rangle$ obtained for $\Gamma_S = 1$ and the same parameters as in Fig. 2.

transient current is defined by $j_{\beta\sigma}(t) = \langle \frac{d\hat{N}_\beta(t)}{dt}\rangle$, where $\hat{N}_\beta(t)$ counts the total number of electrons in electrode $\beta = N, S$. For instance, $j_{N\sigma}(t)$ simplifies to the standard formula [61]

$$j_{N\sigma}(t) = 2\ \mathrm{Im}\sum_{\mathbf{k}} V_{\mathbf{k}}\langle \hat{d}^\dagger_\sigma(t)\hat{c}_{\mathbf{k}\sigma}(t)\rangle. \tag{15}$$

Assuming the energies of itinerant electrons to be static $\varepsilon_{\mathbf{k}\sigma}(t) = \varepsilon_{\mathbf{k}\sigma}$, one obtains

$$\hat{c}_{\mathbf{k}\sigma}(t) = \hat{c}_{\mathbf{k}\sigma}(0)e^{-i\varepsilon_{\mathbf{k}\sigma}t} - i\int_0^t dt' V_{\mathbf{k}} e^{-i\varepsilon_{\mathbf{k}\sigma}(t-t')}\hat{d}_\sigma(t'), \tag{16}$$

and within the wide-band-limit approximation, it yields

$$j_{N\sigma}(t) = 2\mathrm{Im}\left(\sum_{\mathbf{k}} V_{\mathbf{k}} e^{-i\varepsilon_{\mathbf{k}}t}\langle \hat{d}^\dagger_\sigma(t)\hat{c}_{\mathbf{k}\sigma}(0)\rangle\right) - \Gamma_N n_\sigma(t). \tag{17}$$

Finally, inserting the time-dependent operator $\hat{d}^\dagger_\sigma(t)$ [Eq. (A8)] to Eq. (15), we obtain

$$j_{N\sigma}(t) = -\Gamma_N n_\sigma(t) + \frac{\Gamma_N}{\pi}\,\mathrm{Re}\left(\int_{-\infty}^{\infty} d\omega f_N(\omega)e^{-i\omega t} \times \mathcal{L}^{-1}\left\{\frac{s + i\varepsilon_{-\sigma} + \Gamma_N/2}{(s-s_1)(s-s_2)(s-i\omega)}\right\}(t)\right). \tag{18}$$

To compute the transient current of opposite spin electrons, $j_{N-\sigma}(t)$, one should replace the set of auxiliary parameters (s_1, s_2, s_3, s_4) by the following one (s_3, s_4, s_1, s_2). In particular, for $\varepsilon_\sigma = 0$ we get

$$j_{N\sigma}(t) = \frac{\Gamma_N}{\pi}\int_{-\infty}^{\infty} d\omega f_N(\omega)\left\{e^{-\Gamma_N t/2}\frac{1}{2}\sum_{p=\pm}\frac{\omega_p \sin(\omega_p t) - \frac{\Gamma_N}{2}\cos(\omega_p t)}{\left(\frac{\Gamma_N}{2}\right)^2 + \omega_p^2} + \frac{\Gamma_N\left[\left(\frac{\Gamma_N}{2}\right)^2 + \left(\frac{\Gamma_S}{2}\right)^2 + \omega^2\right]}{\left[\left(\frac{\Gamma_N}{2}\right)^2 + \omega_-^2\right]\left[\left(\frac{\Gamma_N}{2}\right)^2 + \omega_+^2\right]}\right\} - \Gamma_N n_\sigma(t), \tag{19}$$

where $\omega_\pm = \frac{\Gamma_S}{2} \pm \omega$. In absence of the superconducting lead, this formula is identical with the result obtained by means of the nonequilibrium Green's function method.

In Fig. 6, we present transient behavior of the current $j_{N\uparrow}(t)$ induced by an abrupt coupling of the QD to both external leads for $\mu_N = \mu_S = 0$ (i.e., without any bias). Similar to the time-dependent QD occupancy (Fig. 2), we observe the quantum oscillations of the period $2\pi/\Gamma_S$ exponentially decaying with the envelope coefficient $e^{-\Gamma_N t}$. Large value of the current at $t = 0^+$ (equal to $e\Gamma_N/2h$) is artifact of the wide band limit approximation [19] in presence of abrupt switching, Eq. (2). In realistic experimental situations, this effect would not be observed. To check how a smooth (gradual) coupling process does affect our predictions, we have computed the transient currents, assuming the sinusoidal switching profile $V_{\mathbf{k},\mathbf{q}}(t) = \frac{V_{\mathbf{k},\mathbf{q}}}{2}(\sin(\pi\Gamma_N t - \pi/2) + 1)$ for $0 < t \leqslant 1/\Gamma_N$ and keeping constant value $V_{\mathbf{k},\mathbf{q}}$ for $t > 1/\Gamma_N$. We have solved this problem numerically. Some representative results (for $\Gamma_N/\Gamma_S = 0.1$) are displayed in the inset in Fig. 6. We noticed that for $t > 1/\Gamma_N$ all the time-dependent quantities are not particularly affected. The only difference (in comparison to the abrupt coupling) is in the early time region $0 < t < 1/\Gamma_N$. For instance, the transient current $j_{N\uparrow}(t)$ smoothly evolves from zero to its asymptotic behavior with the same period of quantum oscillations.

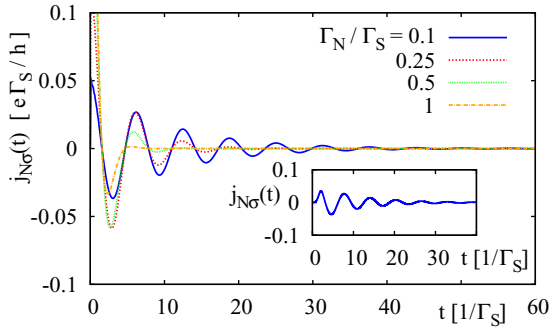

FIG. 6. Transient current between the QD and the normal lead induced by a sudden coupling in absence of any bias. Results are obtained for the same parameters as in Fig. 2. The inset shows the transient current obtained for the sinusoidal coupling profiles $V_{\mathbf{k},\mathbf{q}}(t)$, assuming $\Gamma_N/\Gamma_S = 0.1$.

In similar steps, we have also determined the transient current $j_{S\sigma}(t) = 2\ \mathrm{Im}\sum_{\mathbf{k}} V_{\mathbf{q}}\langle \hat{d}^\dagger_\sigma(t)\hat{c}_{\mathbf{q}\sigma}(t)\rangle$. Effective quasiparticles in superconductors are represented by a coherent superposition of the particle and hole degrees of freedom, so for this reason the time-dependent operator $\hat{c}_{\mathbf{q}\sigma}(t)$ consists of four contributions [see Eq. (A10)]. Final expression for $j_{S\sigma}(t)$ becomes rather lengthy, therefore we present it in Appendix A 4. However, in absence of external voltage the current Eq. (A26) simplifies to

$$j_{S\sigma}(t) = \frac{\Gamma_S^2}{2\sqrt{\delta}}\sin(\sqrt{\delta}t)e^{-\Gamma_N t}\left[1 - \sum_{\sigma'} n_{\sigma'}(0)\right]. \tag{20}$$

When the QD is initially empty/full the transient current $j_{S\sigma} = \pm\frac{\Gamma_S^2}{2\sqrt{\delta}}\sin(\sqrt{\delta}t)e^{-\Gamma_N t}$ reveals the damped oscillations. Contrary to this behavior, for the initial occupancies $n_\sigma(0) = 0$ and $n_{-\sigma}(0) = 1$ the current Eq. (20) vanishes. We assign this

feature to inefficiency of the proximity effect whenever the QD is singly occupied, because electron pairing operates only by mixing the empty with the doubly occupied QD configurations. Initial conditions have thus important influence on transient phenomena.

Furthermore, Eq. (A21) for $\langle \hat{d}_\downarrow(t)\hat{d}_\uparrow(t)\rangle$ and Eq. (A26) imply the exact relationship $j_{S\sigma}(t) = -\Gamma_S \mathrm{Im}\langle \hat{d}_\downarrow \hat{d}_\uparrow\rangle$, which is popular in considerations of charge transport through Josephson junctions [62]. The transient current $j_{S\sigma}(t)$ can hence be simply inferred from Fig. 4. At this point we emphasize that the charge conservation of our heterostructure is properly satisfied:

$$\frac{d}{dt} n_\sigma(t) = j_{S\sigma}(t) + j_{N\sigma}(t) \equiv j_{\mathrm{dis},\sigma}(t), \tag{21}$$

where $j_{\mathrm{dis},\sigma}(t)$ stands for the transient displacement current (see, e.g., Refs. [19,22]).

D. Transient currents for biased system

We have seen so far that time-dependent QD occupancy and transient currents provide indirect information about the subgap quasiparticle energies and dynamical transitions between them. In absence of any voltage ($\mu_N = \mu_S = 0$), these transient currents finally vanish, with a rate dependent on the relaxation processes caused by the coupling Γ_N with a continuum of metallic lead. From the practical point of view, a much more convenient way for probing the timescales characteristic for the Andreev/Shiba quasiparticles could be provided by transient properties of the biased system $\mu_N \neq \mu_S$. Following the steps discussed in previous Sec. III C, we shall study here the time-dependent differential conductance $G_\sigma(\mu, t) \equiv \frac{d}{d\mu} j_{N\sigma}(t)$ as a function of external voltage $\mu \equiv \mu_N$ (throughout this paper, the superconducting lead is assumed to be grounded $\mu_S = 0$). At zero temperature, Eq. (18) implies

$$G_\sigma(\mu,t) = \Gamma_N\, \mathrm{Re}\left[e^{-i\mu t}\mathcal{L}^{-1}\left\{ \frac{s + i\varepsilon_{-\sigma} + \Gamma_N/2}{(s-s_1)(s-s_2)(s-i\mu)} \right\}(t)\right] - \frac{\Gamma_N^2}{2}\, \mathcal{L}^{-1}\left\{ \frac{s + i\varepsilon_{-\sigma} + \Gamma_N/2}{(s-s_1)(s-s_2)(s-i\mu)} \right\}(t)\ \mathcal{L}^{-1}$$
$$\times \left\{ \frac{s - i\varepsilon_{-\sigma} + \Gamma_N/2}{(s-s_3)(s-s_4)(s+i\mu)} \right\}(t) + \frac{\Gamma_N^2\Gamma_S^2}{8}\, \mathcal{L}^{-1}\left\{ \frac{1}{(s-s_1)(s-s_2)(s+i\mu)} \right\}(t)\, \mathcal{L}^{-1}\left\{ \frac{1}{(s-s_3)(s-s_4)(s-i\mu)} \right\}(t), \tag{22}$$

where the conductance is expressed in units of $\frac{2e^2}{h}$. Expression for $G_\downarrow(\mu, t)$ can be obtained by the replacement $(s_1, s_2, s_3, s_4) \to (s_3, s_4, s_1, s_2)$. Using the corresponding inverse Laplace transforms, we find (for $\varepsilon_\sigma = 0$, $G_\uparrow = G_\downarrow = G$)

$$G(\mu,t) = \Gamma_N \left\{ \frac{e^{-\Gamma_N t/2}}{2} \sum_{p=+,-} \frac{\mu_p \sin(\mu_p t) - \frac{\Gamma_N}{2}\cos(\mu_p t)}{\left(\frac{\Gamma_N}{2}\right)^2 + \mu_p^2} + \frac{\left(\frac{\Gamma_N}{2}\right)\left[\left(\frac{\Gamma_N}{2}\right)^2 + \left(\frac{\Gamma_S}{2}\right)^2 + \mu^2\right]}{\left[\left(\frac{\Gamma_N}{2}\right)^2 + \mu_+^2\right]\left[\left(\frac{\Gamma_N}{2}\right)^2 + \mu_-^2\right]} \right\} - \frac{\Gamma_N^2}{2} F_1(\mu,t) + \frac{\Gamma_N^2\Gamma_S^2}{8} F_2(\mu,t), \tag{23}$$

where $F_1(\mu, t)$ and $F_2(\mu, t)$ are given in Eqs. (A15) and (A16), and $\mu_{+/-} = \mu \pm \Gamma_S/2$. In the steady limit, $t \to \infty$ and for $\varepsilon_\sigma = 0$, keeping only terms that survive at late times, we obtain the expression identical with the result derived for the same setup within the Büttiker-Landauer approach [63]

$$G(\mu,\infty) = \frac{\Gamma_N^2\Gamma_S^2}{4\left[\left(\frac{\Gamma_N}{2}\right)^2 + \mu_-^2\right]\left[\left(\frac{\Gamma_N}{2}\right)^2 + \mu_+^2\right]}. \tag{24}$$

For $\Gamma_S \gg \Gamma_N$, the local extrema of this expression occur at $\mu = \pm\frac{\Gamma_S}{2}$ and they correspond to the energies of subgap bound states. For an arbitrary set of model parameters, such information is encoded in Eq. (22) which quantitatively specifies development of the in-gap states driven by the sudden switching at $t = 0$. In Fig. 7, we present the differential conductance obtained numerically for $\Gamma_N/\Gamma_S = 0.1$ and 0.7. Let us notice that differential conductance approaches its steady-limit shape $G_\uparrow(\mu, t = \infty)$ characterized by two Lorentzian quasiparticle peaks centered at $\sim \pm\frac{\Gamma_S}{2}$. Their broadening Γ_N is related to the inverse lifetime.

More careful examination of $G_\uparrow(\mu, t)$ indicates that development of the subgap quasiparticles proceeds in three steps with typical timescales τ_1, τ_2 and τ_f, as can be deduced from Figs. 7 and 8. In Fig. 8, we show how the position of the quasiparticle maxima develops in time for different Γ_N. At $t = \tau_1$, there emerge two maxima from the single broad structure where τ_1 changes approximately from 5 (for $\Gamma_N = 0.2$) up to 10 (for $\Gamma_N = 0.9$) units of time. These maxima move rapidly (essentially during 1–2 units) from $\mu = 0$ up to some value of μ which depends on Γ_N. Next, the position of the quasiparticle peaks evolve continuously to their steady-limit position $\mu = \pm\sqrt{\Gamma_S^2 - \Gamma_N^2}$ with τ_2 approximately changing from 15 (for $\Gamma_N = 0.9$) up to 30 (for $\Gamma_N = 0.2$) units of time. Finally, the asymptotic quasiparticle feature is achieved with the evolve function $1 - \exp(-t/\tau_f)$ where $\tau_f = 2/\Gamma_N$, see Eqs. (23), (A15), and (A16), where the terms proportional to $\exp(-\Gamma_N t/2)$ are responsible for such asymptotic behavior. We also clearly see that, near the quasiparticle peaks, the total differential conductance $\sum_\sigma G(\mu, t \to \infty)$ acquires its optimal value $4e^2/h$ known from the previous studies (see, e.g., Ref. [2]).

IV. CORRELATION EFFECTS

Local repulsive interactions $U\hat{n}_\uparrow\hat{n}_\downarrow$ compete with the proximity-induced electron pairing. This issue has been addressed in the steady limit by numerous methods [2]. In particular, it has been shown [64] that effective pairing (manifested by the in-gap states) is predominantly sensitive to the ratio U/Γ_S and depends on the energy level ε_σ. Various

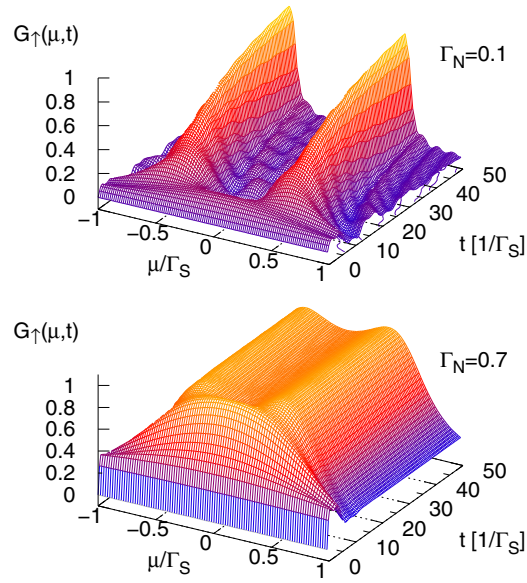

FIG. 7. The time-dependent differential conductance $G_\uparrow(\mu,t) = G_\downarrow(\mu,t)$ (in units of $\frac{4e^2}{h}$) obtained for $\varepsilon_\sigma = 0$, $\Gamma_N = 0.1$ (top panel) and $\Gamma_N = 0.7$ (bottom panel).

experimental realizations of the correlated QD in N-QD-S geometry [57,58,65,66] indicated that the Coulomb potential U safely exceeds (at least one order of magnitude) the superconducting energy gap Δ. Under such circumstances, the correlation effects show up in the subgap regime $|\omega| < \Delta$ merely by a quantum phase transition (or crossover) from the spinless (BCS-type) state $u|0\rangle + v|\uparrow\downarrow\rangle$ to the spinful (singly occupied) configuration $|\sigma\rangle$. This changeover occurs upon increasing the ratio U/Γ_S and, above some critical value of the Coulomb potential $U_{\rm cr}$, there can be observed the subgap Kondo effect (even in the superconducting atomic limit) [66,67]. We shall briefly analyze some correlation effects, focusing on the transient effects.

A. Competition between pairing and correlations

The aforementioned quantum phase transition can be qualitatively captured already within the lowest order

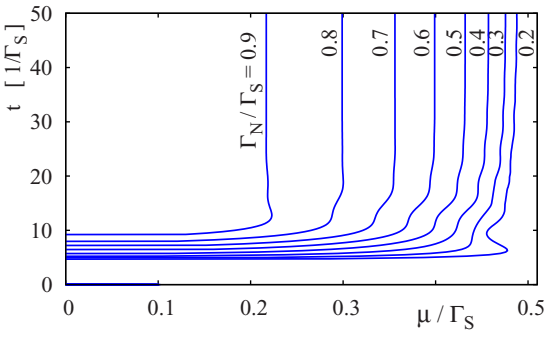

FIG. 8. Positions of the quasiparticle maxima vs. time and μ/Γ_S appearing in the differential conductance $G_\uparrow(\mu,t)$ for a number of ratios Γ_N/Γ_S, as indicated. For negative values of μ/Γ_S the results are symmetrical.

(Hartree-Fock-Bogoliubov) decoupling scheme:

$$\hat{d}^\dagger_\uparrow\hat{d}_\uparrow\hat{d}^\dagger_\downarrow\hat{d}_\downarrow \simeq n_\uparrow(t)\hat{d}^\dagger_\downarrow\hat{d}_\downarrow + n_\downarrow(t)\hat{d}^\dagger_\uparrow\hat{d}_\uparrow - n_\uparrow(t)n_\downarrow(t) + \chi^*(t)\hat{d}^\dagger_\uparrow\hat{d}^\dagger_\downarrow + \chi(t)\hat{d}_\downarrow\hat{d}_\uparrow - |\chi(t)|^2. \quad (25)$$

Using this approximation Eq. (25) one can incorporate the Hartree-Fock terms into the renormalized energy level $\tilde{\epsilon}_\sigma \equiv \epsilon_\sigma + Un_{-\sigma}(t)$, whereas the anomalous (pair source and drain) terms rescale the effective pairing potential $\tilde{\Gamma}_S/2 \equiv \Gamma_S/2 + U\chi(t)$. This decoupling procedure Eq. (25) can give a crossing of the subgap quasiparticle energies at some critical ratio U/Γ_S, dependent also on ε_σ. In the Josephson junctions, such effect would cause a reversal of the dc tunneling current, the so-called $0-\pi$ transition [62,68]. In our N-QD-S heterostructure, its influence is noticeable but rather less spectacular.

Analytical determination of the dynamical observables (discussed in Sec. III) is unfortunately not feasible in the present case, because the renormalized energy level $\tilde{\varepsilon}_\sigma(t)$ and effective pairing potential $\tilde{\Gamma}_S(t)$ are time-dependent in a nonexplicit way and the method used in the previous section is useful only for consideration of systems with constant QD energy levels and couplings with the leads. Therefore, in what follows, we consider the Coulomb repulsion in the system of the proximitized QD coupled only to the normal lead, applying the Hartree-Fock-Bogoliubov approximation Eq. (25). We have computed numerically $n_\sigma(t)$, $\langle\hat{d}_\downarrow(t)\hat{d}_\uparrow(t)\rangle$ and $j_{N\sigma}(t)$, solving the closed set of differential equations for time-dependent functions $n_\sigma(t)$ and $\langle\hat{d}_\downarrow(t)\hat{d}_\uparrow(t)\rangle$, respectively (see Appendix B). At intermediate steps, we had to compute additionally the expectation values $\langle\hat{d}^\dagger_\sigma(t)c_{\mathbf{k}\sigma}(0)\rangle$ and $\langle\hat{d}_\sigma(t)\hat{c}_{\mathbf{k}-\sigma}(0)\rangle$. All these quantities have been determined within the Runge-Kutta numerical algorithm.

Figure 9 displays influence of the Coulomb potential U on the induced order parameter $\chi(t)$ for the unbiased system. The imaginary part, which is strictly related to the transient current, exhibits the damped quantum oscillations. Their period and amplitude are substantially suppressed by the Coulomb potential. We assign this fact to a competition between the on-dot pairing and local Coulomb repulsion. The real part of $\chi(t)$ is characterized by the same quantum oscillations. The asymptotic value of the complex order parameter $\chi(t\to\infty)$ with respect to the Coulomb potential U is shown in Fig. 10 for $\varepsilon_\sigma = 0$, $\Gamma_N/\Gamma_S = 0.2$. Such monotonously decreasing ${\rm Re}\chi(\infty)$ confirms a competing relationship between the on-dot pairing and the local repulsion.

In Fig. 11, we show influence of the Coulomb potential U on the QD occupancy $n_\uparrow(t)$. Besides the quantum oscillations, similar to the ones observed in the complex order parameter (Fig. 9), we notice a partial reduction of the QD charge upon increasing U. Apparently, this is caused by the Hartree term $Un_{-\sigma}(t)$ that lifts the renormalized QD level $\tilde{\varepsilon}_\sigma(t)$. In the next subsection we briefly discuss the time-dependent subgap Kondo effect.

B. Subgap Kondo effect

In this subsection, we briefly discuss another characteristic timescale, which could be related to the subgap Kondo effect. Since we cannot account for this effect within the equation of motion approach, we make some conjectures based on

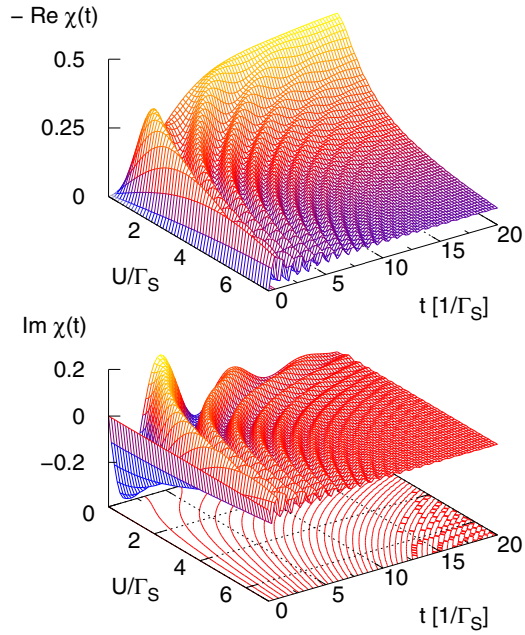

FIG. 9. Influence of the Coulomb potential U on the real (upper panel) and imaginary (bottom panel) parts of the induced pairing $\chi(t) = \langle \hat{d}_\downarrow \hat{d}_\uparrow \rangle$ obtained for the unbiased system, using $\varepsilon_\sigma = 0$, $\Gamma_N = 0.2$ and $\Gamma_S \equiv 1$.

(i) systematic study of the steady case [66–68] combined with (ii) time-dependent analysis of the Kondo physics of normal QDs [35]. Self-consistent treatment of this phenomenon, which is beyond the scope of the present paper, would be very much welcome.

When the Coulomb potential U is sufficiently large in comparison to Γ_S, the QD ground state evolves towards the spinful (doublet) configuration $|\sigma\rangle$. Under such conditions, the effective spin exchange between the correlated QD and mobile electrons of the metallic lead activate the subgap Kondo effect. It has been analyzed by many groups, using various techniques [2]. In the present context, we shall make use of basic facts pointed out recently by R. Žitko *et al.* [66] and independently by one of us [67,68].

The exchange interaction $-\sum_{\mathbf{k},\mathbf{p}} J_{\mathbf{k},\mathbf{p}}\ \hat{\mathbf{S}}_d \cdot \hat{\mathbf{S}}_{\mathbf{kp}}$ between the QD spin $\hat{\mathbf{S}}_d$ and spins $\hat{\mathbf{S}}_{\mathbf{kp}}$ of the mobile electrons in the normal lead can be determined by means of the generalizing canonical

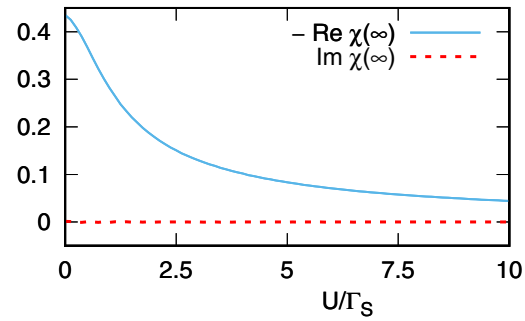

FIG. 10. Asymptotic value of complex on-dot pairing $\chi(t \to \infty)$ suppressed by the Coulomb repulsion U obtained for the same model parameters as in Fig. 9.

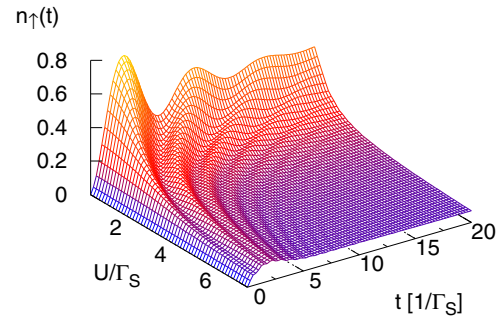

FIG. 11. The time-dependent occupancy of the correlated quantum dot for $\epsilon_\sigma = 0$, $\Gamma_N = 0.2$, $\Gamma_S = 1$ in absence of external voltage.

Schrieffer-Wolff transformation. Adopting it to the N-QD-S setup, it has been found that for the superconducting atomic limit, the exchange coupling near the Fermi energy $J_{\mathbf{k}_F,\mathbf{k}_F}$ is equal to [67]

$$J_{\mathbf{k}_F,\mathbf{k}_F} = \frac{U|V_{\mathbf{k}_F}|^2}{\varepsilon_\sigma(\varepsilon_\sigma + U) + (\Gamma_S/2)^2}. \tag{26}$$

For a spinful configuration, the Kondo temperature can be estimated, e.g., using the Bethe-Ansatz formula $T_K \propto \exp\{-1/[2\rho(\varepsilon_F)J_{\mathbf{k}_F\mathbf{k}_F}]\}$, where $\rho(\varepsilon_F)$ is the density of states of the normal lead at the Fermi level. We have compared such results with the unbiased NRG calculations and it has been found that the Kondo temperature is expressed by [67]

$$T_K = \eta\, \frac{\sqrt{\Gamma_N U}}{2}\, \exp\left[\pi\, \frac{\varepsilon_\sigma(\varepsilon_\sigma + U) + (\Gamma_S/2)^2}{\Gamma_N U}\right], \tag{27}$$

with $\eta \approx 0.6$. In particular, for the half-filled QD ($\varepsilon_\sigma = -U/2$), the exchange coupling Eq. (26) simplifies to

$$J_{\mathbf{k}_F,\mathbf{k}_F} = J^{(N)}_{\mathbf{k}_F,\mathbf{k}_F}\, \frac{U^2}{U^2 - \Gamma_S^2}, \tag{28}$$

where $J^{(N)}_{\mathbf{k}_F,\mathbf{k}_F}$ stands for the normal case ($\Gamma_S = 0$). Upon approaching a transition from the spinful doublet to the BCS-like (spinless) ground state, the Kondo temperature is substantially enhanced [66,67]

$$T_K = T_K^{(N)} \exp\left[\frac{\pi}{\Gamma_N U}\left(\frac{\Gamma_S}{2}\right)^2\right]. \tag{29}$$

To get some insight into the transient phenomena related with the subgap Kondo regime, we make use of the final conclusions inferred in Ref. [35] from the time-dependent noncrossing approximation study. The characteristic time τ_K needed for the Abrikosov-Suhl peak to emerge at the Fermi level has been found to scale inversely with the Kondo temperature, i.e., $\tau_K \sim 1/T_K$. This information adopted to our N-QD-S setup implies the following relative ratio for the half-filled QD:

$$\tau_K = \tau_K^{(N)} \exp\left[-\frac{\pi}{\Gamma_N U}\left(\frac{\Gamma_S}{2}\right)^2\right], \tag{30}$$

where $\tau_K^{(N)}$ stands for the normal state value ($\Gamma_S = 0$). We plot this scaling in Fig. 12. Let us remark that many-body screening, Eq. (26), of the QD spin can be practically realized only in the

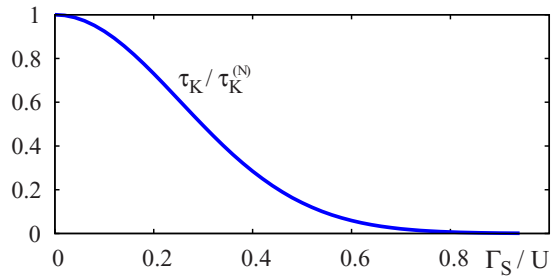

FIG. 12. Characteristic timescale $\tau_K \sim 1/T_K$ of the subgap Kondo effect obtained for the half-filled QD using $U = 10\Gamma_N$ with respect to varying ratio Γ_S/U. In this case, the spinful ground state exists in the region $\Gamma_S \in (0, U)$.

doublet ground state (which for the half-filled QD occurs when $\Gamma_S < U$). By increasing the ratio Γ_S/U, the Andreev bound states tend to their crossing and simultaneously the Abrikosov-Suhl peak Eq. (29) quickly broadens [66,67]. This explains why the characteristic timescale τ_K strongly decreases with respect to Γ_S/U.

V. SUMMARY

We have investigated transient effects driven by a sudden coupling of the QD to the metallic and superconducting leads. Our study has revealed a gradual buildup of the subgap Andreev quasiparticle states, which is controlled by the coupling Γ_N to a continuous spectrum of the metallic lead. Depending on the initial QD occupancy, we have also found the damped quantum oscillations of the charge occupancy $n_\sigma(t)$, the complex order parameter $\chi(t)$, and the transient currents $j_{N\sigma}(t)$, $j_{S\sigma}(t)$. A period of these oscillations would be sensitive to the Andreev quasiparticle energies, which can be indirectly controlled via a coupling Γ_S to the superconducting reservoir.

Analogous effects (relaxation and quantum oscillations) have been recently reported in Refs. [9,51] in studies of the metastable subgap states for the Josephson junction, considering finite value of the superconducting gap. We estimate that in realistic systems, where $\Gamma_S \sim 0.2$ meV, the period of quantum oscillations would be a fraction of nanoseconds or in picoseconds regime (hence should be empirically detectable). Buildup of the subgap Andreev quasiparticle states is expected to be formed in N-QD-S junctions on a much longer timescale, corresponding to a microsecond regime. Our estimations seem to reliable, when comparing them with dynamical transitions between the subgap bound states of nanotubes [8] and parity switchings observed in the superconducting atomic contacts [69].

We also addressed the correlation effects by means of the Hartree-Fock-Bogoliubov approximation, revealing that the repulsive Coulomb potential U suppresses the proximity-induced electron pairing. We have explored some time-dependent signatures of this competition. In particular, we have found that Γ_N controls the rate at which the stationary limit behavior is achieved, whereas the period of the damped quantum oscillations is dependent on the Coulomb potential due to its influence of the Andreev quasiparticle energies [64].

Finally, we have tried to evaluate the characteristic timescale τ_K needed for the subgap Kondo effect to develop. Upon approaching the quantum phase transition from the (spinful) doublet side, we predict the strong reduction of this scale τ_K, originating from a subtle interplay between the induced on-dot pairing and the Coulomb repulsion [66,67]. We hope that such variety of dynamical effects of the proximitized QDs could be verified experimentally.

ACKNOWLEDGMENTS

We acknowledge instructive discussions with V. Janiš and thank A. Baumgartner for useful remarks on observability of the transient effects in multiterminal heterostructures. We also kindly thank T. Kwapiński for technical assistance. This work is supported by the National Science Centre (NCN, Poland) through Grants No. DEC-2014/13/B/ST3/04451 (T.D.) and No. UMO-2017/27/B/ST3/01911 (R.T.).

APPENDIX A

In this Appendix, we derive the Laplace transforms $\hat{d}_\sigma(s)$ and $\hat{c}_{\mathbf{q}\sigma}(s)$, which are needed for calculating the statistically averaged physical quantities discussed in this work. We present explicit formulas for the QD occupancy, the pair correlation function, and the transient currents flowing between QD and external reservoirs for the case $\Delta = \infty$ and $U = 0$.

1. Laplace transforms

To calculate expectation values of the quantities studied in this paper, we need the time-dependent operator $\hat{d}_\sigma(t)$. We can obtain it by computing the corresponding inverse Laplace transform $\mathcal{L}^{-1}\{\hat{d}_\sigma(s)\}(t)$. To determine $\hat{d}_\sigma(s)$, we use a closed set of the equations of motion for the operators: $\hat{d}_\sigma(t), \hat{d}^\dagger_{-\sigma}(t)$, $\hat{c}_{\mathbf{k}\sigma}(t)$, $\hat{c}^\dagger_{\mathbf{k}-\sigma}(t), \hat{c}_{\mathbf{q}\sigma}(t)$, $\hat{c}^\dagger_{-\mathbf{q}-\sigma}(t)$, $\hat{c}^\dagger_{\mathbf{q}-\sigma}(t)$, and $\hat{c}_{-\mathbf{q}\sigma}(t)$. Laplace transforms of these differential equations for $\sigma = \uparrow$ (assuming arbitrary energy gap Δ and neglecting the correlations) take the following form:

$$(s + i\varepsilon_\uparrow)\hat{d}_\uparrow(s) = -i\sum_{\mathbf{k/q}} V_{\mathbf{k/q}}\hat{c}_{\mathbf{k/q}\uparrow}(s) + \hat{d}_\uparrow(0), \tag{A1a}$$

$$(s + i\varepsilon_{\mathbf{k}})\hat{c}_{\mathbf{k}\uparrow}(s) = -iV_{\mathbf{k}}\hat{d}_\uparrow(s) + \hat{c}_{\mathbf{k}\uparrow}(0), \tag{A1b}$$

$$(s + i\varepsilon_{\mathbf{q}})\hat{c}_{\mathbf{q}\uparrow}(s) = -iV_{\mathbf{q}}\hat{d}_\uparrow(s) - i\Delta\hat{c}^\dagger_{-\mathbf{q}\downarrow}(s) + \hat{c}_{\mathbf{q}\uparrow}(0), \tag{A1c}$$

$$(s - i\varepsilon_{\mathbf{q}})\hat{c}^\dagger_{-\mathbf{q}\downarrow}(s) = iV_{\mathbf{q}}\hat{d}^\dagger_\downarrow(s) - i\Delta\hat{c}_{\mathbf{q}\uparrow}(s) + \hat{c}^\dagger_{-\mathbf{q}\downarrow}(0), \tag{A1d}$$

$$(s - i\varepsilon_\downarrow)\hat{d}^\dagger_\downarrow(s) = i\sum_{\mathbf{k/q}} V_{\mathbf{k/q}}\hat{c}^\dagger_{\mathbf{k/q}\downarrow}(s) + \hat{c}^\dagger_\downarrow(0), \tag{A1e}$$

$$(s - i\varepsilon_{\mathbf{k}})\hat{c}^\dagger_{\mathbf{k}\downarrow}(s) = iV_{\mathbf{k}}\hat{d}^\dagger_\downarrow(s) + \hat{c}^\dagger_{\mathbf{k}\downarrow}(0), \tag{A1f}$$

$$(s - i\varepsilon_{\mathbf{q}})\hat{c}^\dagger_{\mathbf{q}\downarrow}(s) = iV_{\mathbf{q}}\hat{d}^\dagger_\downarrow(s) - i\Delta\hat{c}_{-\mathbf{q}\uparrow}(s) + \hat{c}^\dagger_{\mathbf{q}\downarrow}(0), \tag{A1g}$$

$$(s + i\varepsilon_{\mathbf{q}})\hat{c}_{-\mathbf{q}\uparrow}(s) = -iV_{\mathbf{q}}\hat{d}_\uparrow(s) - i\Delta\hat{c}^\dagger_{\mathbf{q}\downarrow}(s) - \hat{c}_{-\mathbf{q}\uparrow}(0). \tag{A1h}$$

Here we have assumed $\varepsilon_{\mathbf{q}\sigma} = \varepsilon_{\mathbf{q}}$, $\varepsilon_{\mathbf{q}} = \varepsilon_{-\mathbf{q}}$ and the subscript $\mathbf{k}(\mathbf{q})$ corresponds to the normal (superconducting) electrode.

To obtain $\hat{d}_\uparrow(s)$, we have to calculate $\hat{c}^\dagger_{-\mathbf{q}\downarrow}(s)$ from Eq. (A1d) and insert it into Eq. (A1c) for the operator $\hat{c}_{\mathbf{q}\uparrow}(s)$. In a next step, we use $\hat{c}_{\mathbf{q}\uparrow}(s)$ in the expression for $\hat{d}_\uparrow(s)$ given in Eq. (A1a) along with $\hat{c}_{\mathbf{k}\uparrow}(s)$ obtained from Eq. (A1b). In consequence, we get

$$\hat{d}_\uparrow(s) M^{(+)}_\uparrow(s) = \hat{A}(s) - iK(s)\hat{d}^\dagger_\downarrow(s). \tag{A2}$$

Next, we repeat this procedure, Eqs. (A1e)–(A1h), obtaining

$$\hat{d}^\dagger_\downarrow(s) M^{(-)}_\downarrow(s) = \hat{B}(s) - iK(s)\hat{d}_\uparrow(s), \tag{A3}$$

where

$$M^{(\pm)}_\sigma(s) = s \pm i\varepsilon_\sigma + \sum_{\mathbf{k}} \frac{V^2_{\mathbf{k}}}{s \pm i\varepsilon_{\mathbf{k}}} + \sum_{\mathbf{q}} \frac{V^2_{\mathbf{q}}(s \mp i\varepsilon_{\mathbf{q}})}{s^2 + \varepsilon^2_{\mathbf{q}} + \Delta^2}, \tag{A4}$$

$$K(s) = \sum_{\mathbf{q}} \frac{V^2_{\mathbf{q}}\,\Delta}{s^2 + \varepsilon^2_{\mathbf{q}} + |\Delta|^2}, \tag{A5}$$

$$\hat{A}(s) = -i \sum_{\mathbf{k}} \frac{V_{\mathbf{k}}\,\hat{c}_{\mathbf{k}\uparrow}(0)}{s + i\varepsilon_{\mathbf{k}}} - \sum_{\mathbf{q}} \frac{V_{\mathbf{q}}}{s^2 + \varepsilon^2_{\mathbf{q}} + \Delta^2}(\Delta \hat{c}^\dagger_{-\mathbf{q}\downarrow}(0) + i(s - i\varepsilon_{\mathbf{q}})\hat{c}_{\mathbf{q}\uparrow}(0)) + \hat{d}_\uparrow(0), \tag{A6}$$

$$\hat{B}(s) = i \sum_{\mathbf{k}} \frac{V_{\mathbf{k}}\hat{c}^\dagger_{\mathbf{k}\downarrow}(0)}{s - i\varepsilon_{\mathbf{k}}} + \sum_{\mathbf{q}} \frac{V_{\mathbf{q}}}{s^2 + \varepsilon^2_{\mathbf{q}} + \Delta^2}(\Delta \hat{c}_{-\mathbf{q}\uparrow}(0) + i(s + i\varepsilon_{\mathbf{q}})\hat{c}^\dagger_{\mathbf{q}\downarrow}(0)) + \hat{d}^\dagger_\downarrow(0). \tag{A7}$$

Equations (A2) and (A3) yield

$$\hat{d}_\uparrow(s) = \frac{M^{(-)}_\downarrow(s)\hat{A}(s) - iK(s)\hat{B}(s)}{M^{(+)}_\uparrow(s)M^{(-)}_\downarrow(s) + K^2(s)}. \tag{A8}$$

To determine $\hat{d}_\downarrow(s)$, one should repeat the same procedure for a set of equations of motion for the operators: $\hat{d}_\downarrow$, $\hat{d}^\dagger_\uparrow$, $\hat{c}_{\mathbf{k}\downarrow}$, $\hat{c}^\dagger_{\mathbf{k}\uparrow}$, $\hat{c}_{\mathbf{q}\downarrow}$, $\hat{c}^\dagger_{-\mathbf{q}\uparrow}$, $\hat{c}^\dagger_{\mathbf{q}\uparrow}$ and $\hat{c}^\dagger_{-\mathbf{q}\downarrow}(t)$, respectively. Effectively, we get

$$\hat{d}_\downarrow(s) = \frac{M^{(-)}_\uparrow(s)\hat{B}^\dagger(s) + iK(s)\hat{A}^\dagger(s)}{M^{(+)}_\downarrow(s)M^{(-)}_\uparrow(s) + K^2(s)}. \tag{A9}$$

In similar steps, we can compute $\hat{c}_{\mathbf{q}\sigma}(s)$, which is needed in expression for the current flowing between the QD and the superconductor. From Eqs. (A1a)–(A1h), we obtain

$$\hat{c}_{\mathbf{q}\sigma}(s) = \frac{1}{s^2 + \varepsilon^2_{\mathbf{q}} + |\Delta|^2}(-iV_{\mathbf{q}}(s - i\varepsilon_{\mathbf{q}})\hat{d}_\sigma(s) + \alpha\Delta V_{\mathbf{q}}\hat{d}^\dagger_{-\sigma}(s) - i\alpha\Delta\hat{c}^\dagger_{-\mathbf{q}-\sigma}(0) + (s - i\varepsilon_{\mathbf{q}})\hat{c}_{\mathbf{q}\sigma}(0)), \tag{A10}$$

where $\alpha = +(-)$ for $\sigma = \uparrow(\downarrow)$. Laplace transforms of $\hat{d}^\dagger_\sigma(s)$ can be obtained taking the Hermitian conjugate of the operators $\hat{d}_\sigma(s)$ given in Eqs. (A8) and (A9). Note that in the wide-band-limit approximation, the functions $M^{(\pm)}_\sigma(s)$ and $K(s)$ simplify in the superconducting atomic limit $\Delta = \infty$ to $s \pm i\varepsilon_\sigma + \Gamma_N/2$ and $\Gamma_S/2$, respectively. As an example, we present here the explicit form of the Laplace transform for $\hat{d}_\uparrow(t)$:

$$\hat{d}_\uparrow(s) = \frac{1}{(s - s_3)(s - s_4)}\left\{\left(s - i\varepsilon_\downarrow + \frac{\Gamma_N}{2}\right)\left[\hat{d}_\uparrow(0) - i\sum_{\mathbf{k}} \frac{V_{\mathbf{k}}\,\hat{c}_{\mathbf{k}\uparrow}(0)}{s + i\varepsilon_{\mathbf{k}}} - i\sum_{\mathbf{q}} \frac{V_{\mathbf{q}}(s - i\varepsilon_{\mathbf{q}})\hat{c}_{\mathbf{q}\uparrow}(0)}{s^2 + \varepsilon^2_{\mathbf{q}} + \Delta^2} - \sum_{\mathbf{q}} \frac{V_{\mathbf{q}}\Delta\hat{c}^\dagger_{-\mathbf{q}\downarrow}(0)}{s^2 + \varepsilon^2_{\mathbf{q}} + \Delta^2}\right]\right.$$
$$\left. - i\frac{\Gamma_S}{2}\left[\hat{d}^\dagger_\downarrow(0) + i\sum_{\mathbf{k}} \frac{V_{\mathbf{k}}\,\hat{c}^\dagger_{\mathbf{k}\downarrow}(0)}{s - i\varepsilon_{\mathbf{k}}} + i\sum_{\mathbf{q}} \frac{V_{\mathbf{q}}(s + i\varepsilon_{\mathbf{q}})\hat{c}^\dagger_{\mathbf{q}\downarrow}(0)}{s^2 + \varepsilon^2_{\mathbf{q}} + \Delta^2} + \sum_{\mathbf{q}} \frac{V_{\mathbf{q}}\Delta\hat{c}_{-\mathbf{q}\uparrow}(0)}{s^2 + \varepsilon^2_{\mathbf{q}} + \Delta^2}\right]\right\}. \tag{A11}$$

The creation operator $\hat{d}^\dagger_\uparrow(s)$ can be simply obtained from the Hermitian conjugate of Eq. (A11) and using the replacement $(s_3, s_4) \leftrightarrow (s_1, s_2)$. Note, that the operators $\hat{d}_\sigma(s)$ and $\hat{d}^\dagger_\sigma(s)$ depend on the superconducting energy gap Δ. In the main part of this paper, we have focused on the superconducting limit $\Delta \to \infty$, calculating the average values of $\langle \hat{d}^\dagger_\sigma(t)\hat{d}_\sigma(t)\rangle$, $\langle \hat{d}_\sigma(t)\hat{d}_{-\sigma}(t)\rangle$, and $\langle \hat{d}^\dagger_\sigma(t)\hat{c}_{\mathbf{k}'\sigma}(t)\rangle$.

2. QD occupancy

Let us determine the QD occupancy, $n_\sigma(t)$, expressed by the formula Eq. (4) computing expectation value of a product of the corresponding inverse Laplace transforms. Initially, at $t=0$, the QD is decoupled from both external reservoirs, therefore the only nonvanishing terms comprise the following averages $\langle \hat{d}^\dagger_\sigma(0)\hat{d}_\sigma(0)\rangle = n_\sigma(0)$, $\langle \hat{d}_\sigma(0)\hat{d}^\dagger_\sigma(0)\rangle = 1-n_\sigma(0)$, $\langle \hat{c}^\dagger_{\mathbf{k}\sigma}(0)\hat{c}_{\mathbf{k}'\sigma}(0)\rangle = \delta_{\mathbf{k},\mathbf{k}'} f_N(\varepsilon_\mathbf{k})$, and $\langle \hat{c}_{\mathbf{k}\sigma}(0)\hat{c}^\dagger_{\mathbf{k}'\sigma}(0)\rangle = \delta_{\mathbf{k},\mathbf{k}'}[1-f_N(\varepsilon_\mathbf{k})]$, where $f_N(\varepsilon_\mathbf{k})$ is the Fermi-Dirac distribution of the normal lead. Other terms, corresponding to itinerant electrons of the superconducting lead, can be neglected in the limit $\Delta=\infty$, but they could be also included when considering the finite energy gap (we shall return to this issue later on). Using Eq. (A8), we obtain the QD occupancy given by

$$\begin{aligned} n_\sigma(t) &= \mathcal{L}^{-1}\left\{\frac{s+i\varepsilon_{-\sigma}+\frac{\Gamma_N}{2}}{(s-s_1)(s-s_2)}\right\}(t)\mathcal{L}^{-1}\left\{\frac{s-i\varepsilon_{-\sigma}+\frac{\Gamma_N}{2}}{(s-s_3)(s-s_4)}\right\}(t)\ \langle \hat{d}^\dagger_\sigma(0)\hat{d}_\sigma(0)\rangle \\ &+\left(\frac{\Gamma_S}{2}\right)^2 \mathcal{L}^{-1}\left\{\frac{1}{(s-s_1)(s-s_2)}\right\}(t)\mathcal{L}^{-1}\left\{\frac{1}{(s-s_3)(s-s_4)}\right\}(t)\ \langle \hat{d}_{-\sigma}(0)\hat{d}^\dagger_{-\sigma}(0)\rangle \\ &+\left(\frac{\Gamma_S}{2}\right)^2 \sum_{\mathbf{k},\mathbf{k}'} V_\mathbf{k}V_{\mathbf{k}'}\mathcal{L}^{-1}\left\{\frac{1}{(s-s_1)(s-s_2)(s+i\varepsilon_\mathbf{k})}\right\}(t)\mathcal{L}^{-1}\left\{\frac{1}{(s-s_3)(s-s_4)(s-i\varepsilon_{\mathbf{k}'})}\right\}(t)\langle \hat{c}_{\mathbf{k}-\sigma}(0)\hat{c}^\dagger_{\mathbf{k}'-\sigma}(0)\rangle \\ &+\sum_{\mathbf{k},\mathbf{k}'} V_\mathbf{k}V_{\mathbf{k}'}\mathcal{L}^{-1}\left\{\frac{s+i\varepsilon_{-\sigma}+\frac{\Gamma_N}{2}}{(s-s_1)(s-s_2)(s-i\varepsilon_\mathbf{k})}\right\}(t)\mathcal{L}^{-1}\left\{\frac{s-i\varepsilon_{-\sigma}+\frac{\Gamma_N}{2}}{(s-s_3)(s-s_4)(s+i\varepsilon_{\mathbf{k}'})}\right\}(t)\langle \hat{c}^\dagger_{\mathbf{k}\sigma}(0)\hat{c}_{\mathbf{k}'\sigma}(0)\rangle. \end{aligned} \tag{A12}$$

For $\sigma=\downarrow$, one should make the replacement $(s_1,s_2,s_3,s_4)\to(s_3,s_4,s_1,s_2)$. Using the wide-band limit approximation, we can recast summations over momenta of the third and fourth terms in Eq. (A12) by the integrals

$$\begin{aligned} &\frac{\Gamma_S^2}{4}\frac{\Gamma_N}{2\pi}\int_{-\infty}^{\infty} d\varepsilon[1-f_N(\varepsilon)]\mathcal{L}^{-1}\left\{\frac{1}{(s-s_1)(s-s_2)(s+i\varepsilon)}\right\}(t)\mathcal{L}^{-1}\left\{\frac{1}{(s-s_3)(s-s_4)(s-i\varepsilon)}\right\}(t) \\ &+\frac{\Gamma_N}{2\pi}\int_{-\infty}^{\infty} d\varepsilon f_N(\varepsilon)\mathcal{L}^{-1}\left\{\frac{s+i\varepsilon_{-\sigma}+\frac{\Gamma_N}{2}}{(s-s_1)(s-s_2)(s-i\varepsilon)}\right\}(t)\mathcal{L}^{-1}\left\{\frac{s-i\varepsilon_{-\sigma}+\frac{\Gamma_N}{2}}{(s-s_3)(s-s_4)(s+i\varepsilon)}\right\}(t). \end{aligned} \tag{A13}$$

The final formula for $n_\sigma(t)$ is quite lengthy, therefore we present its simpler explicit form, corresponding to $\varepsilon_\sigma=0$:

$$\begin{aligned} n_\sigma(t) &= n_\sigma(0)e^{-\Gamma_N t}+[1-n_\sigma(0)-n_{-\sigma}(0)]e^{-\Gamma_N t}\sin^2\left(\frac{\Gamma_S}{2}t\right) \\ &+\frac{\Gamma_N}{2\pi}\int_{-\infty}^{\infty} d\varepsilon\ f_N(\varepsilon)\ F_1(\varepsilon,t)+\frac{\Gamma_N}{2\pi}\frac{\Gamma_S^2}{4}\int_{-\infty}^{\infty} d\varepsilon\ [1-f_N(\varepsilon)]F_2(\varepsilon,t). \end{aligned} \tag{A14}$$

Functions $F_1(\varepsilon,t)$ and $F_2(\varepsilon,t)$ are defined by

$$\begin{aligned} F_1(\varepsilon,t) &= \frac{1}{A(\varepsilon)}\left\{\frac{\Gamma_N^2}{4}+\varepsilon^2+\frac{e^{-\Gamma_N t}}{2}\left[\left(\frac{\Gamma_N^2}{4}-\frac{\Gamma_S^2}{4}+\varepsilon^2\right)\cos(\Gamma_S t)-\frac{\Gamma_N\Gamma_S}{2}\sin(\Gamma_S t)+\frac{\Gamma_N^2}{4}+\frac{\Gamma_S^2}{4}+\varepsilon^2\right]\right. \\ &\left.-e^{-\Gamma_N t/2}\left[2\left(\frac{\Gamma_N^2}{4}+\varepsilon^2\right)\cos(\varepsilon t)\cos\left(\frac{\Gamma_S}{2}t\right)-\frac{\Gamma_N\Gamma_S}{2}\cos(\varepsilon t)\sin\left(\frac{\Gamma_S}{2}t\right)+\Gamma_S\varepsilon\sin(\varepsilon t)\sin\left(\frac{\Gamma_S}{2}t\right)\right]\right\}, \end{aligned} \tag{A15}$$

$$\begin{aligned} F_2(\varepsilon,t) &= \frac{1}{\Gamma_S A(\varepsilon)}\left\{e^{-\Gamma_N t}\left[\frac{-2}{\Gamma_S}\left(\frac{\Gamma_N^2}{4}-\frac{\Gamma_S^2}{4}+\varepsilon^2\right)\cos(\Gamma_S t)+\Gamma_N\sin(\Gamma_S t)+\frac{2}{\Gamma_S}\left(\frac{\Gamma_N^2}{4}+\frac{\Gamma_S^2}{4}+\varepsilon^2\right)\right]\right. \\ &\left.+e^{-\Gamma_N t/2}[2(\varepsilon_-\cos(\varepsilon_+ t)-\varepsilon_+\cos(\varepsilon_- t))-\Gamma_N(\sin(\varepsilon_+ t)-\sin(\varepsilon_- t))]+\Gamma_S\right\}, \end{aligned} \tag{A16}$$

and $A(\varepsilon)=(\frac{\Gamma_N^2}{4}+\varepsilon_-^2)(\frac{\Gamma_N^2}{4}+\varepsilon_+^2)$, where $\varepsilon_{+/-}=\varepsilon\pm\frac{\Gamma_S}{2}$. It should be noted that for $\Gamma_S=0$ the formula Eq. (A12) coincides with the standard expression

$$n_\sigma(t)=n_\sigma(0)e^{-\Gamma_N t}+\frac{\Gamma_N}{\pi}e^{-\Gamma_N t/2}\int_{-\infty}^{\infty} d\varepsilon\ f_N(\varepsilon)\frac{\cosh(\Gamma_N t/2)-\cos((\varepsilon-\varepsilon_\sigma)t)}{\frac{\Gamma_N^2}{4}+(\varepsilon-\varepsilon_\sigma)^2} \tag{A17}$$

obtained by the nonequilibrium Green's function (NEGF) technique [61]. We are not aware of any results available for $\Gamma_S\neq 0$, but it seems that our approach would be simpler in comparison to the NEGF method in which the QD occupancy is formally

expressed via the lesser Green's function $n_\sigma(t) = -iG^<(t,t)$. In practice, it can be determined from the Keldysh equation

$$G^< = (1 + G^r\Sigma^r)G_0^<(1 + \Sigma^a G^a) + G^r\Sigma^< G^a. \tag{A18}$$

In particular, for $n_\sigma(0) = 0$ Eq. (A18) simplifies to $G^< = G^r\Sigma^< G^a$ (because $G_0^< = 0$ [19,61]). In other cases, however, determination of the lesser Green's function is much more demanding.

We now return to the discussion of the terms appearing in formula Eq. (4), which contain the operators $\hat{c}_{\mathbf{q}\sigma}$. Let us analyze one of such terms, e.g.,

$$\left\langle \mathcal{L}^{-1}\left\{\frac{s+i\varepsilon_\downarrow+\frac{\Gamma_N}{2}}{(s-s_1)(s-s_2)}\sum_{\mathbf{q}}\frac{V_{\mathbf{q}}(s+i\varepsilon_{\mathbf{q}})\hat{c}^\dagger_{\mathbf{q}\uparrow}(0)}{s^2+\varepsilon_{\mathbf{q}}^2+\Delta^2}\right\}(t)\mathcal{L}^{-1}\left\{\frac{s-i\varepsilon_\downarrow+\frac{\Gamma_N}{2}}{(s-s_3)(s-s_4)}\sum_{\mathbf{q}'}\frac{V_{\mathbf{q}'}(s-i\varepsilon_{\mathbf{q}'})\hat{c}_{\mathbf{q}'\uparrow}(0)}{s^2+\varepsilon_{\mathbf{q}'}^2+\Delta^2}\right\}(t)\right\rangle, \tag{A19}$$

which can be reduced to the form

$$\frac{\Gamma_S}{2\pi}\int_{-\infty}^{+\infty}d\varepsilon f_S(\varepsilon)\mathcal{L}^{-1}\left\{\frac{\left(s+i\varepsilon_\downarrow+\frac{\Gamma_N}{2}\right)(s+i\varepsilon)}{(s-s_1)(s-s_2)(s^2+\varepsilon^2+\Delta^2)}\right\}(t)\mathcal{L}^{-1}\left\{\frac{\left(s-i\varepsilon_\downarrow+\frac{\Gamma_N}{2}\right)(s-i\varepsilon)}{(s-s_3)(s-s_4)(s^2+\varepsilon^2+\Delta^2)}\right\}(t), \tag{A20}$$

where we made use of the equality $\langle\hat{c}^\dagger_{\mathbf{q}\uparrow}(0)\hat{c}_{\mathbf{q}'\uparrow}(0)\rangle = \delta_{\mathbf{q}\mathbf{q}'}f_s(\varepsilon_{\mathbf{q}})$. We have checked (by numerically integrating the product of the corresponding inverse Laplace transforms) that this integral becomes smaller and smaller upon increasing Δ, and it finally diminishes to zero in the limit $\Delta = \infty$. Similarly, we have checked that all other terms comprising the operators $\hat{c}_{\mathbf{q}\sigma}(0)$ disappear for $\Delta = \infty$ as well.

3. QD pair correlation function

Using the explicit formulas for $\hat{d}_\sigma(s)$, presented in Eqs. (A8) and (A9) and performing similar calculations as for the QD occupancy, we obtained the induced on-dot pairing given by

$$\begin{aligned}\langle\hat{d}_\downarrow(t)\hat{d}_\uparrow(t)\rangle = i\frac{\Gamma_S}{2}\Bigg[&n_\uparrow(0)\,\mathcal{L}^{-1}\left\{\frac{1}{(s-s_1)(s-s_2)}\right\}(t)\mathcal{L}^{-1}\left\{\frac{s-i\varepsilon_\downarrow+\frac{\Gamma_N}{2}}{(s-s_3)(s-s_4)}\right\}(t)\\
&-(1-n_\downarrow(0))\,\mathcal{L}^{-1}\left\{\frac{s-i\varepsilon_\uparrow+\frac{\Gamma_N}{2}}{(s-s_1)(s-s_2)}\right\}(t)\mathcal{L}^{-1}\left\{\frac{1}{(s-s_3)(s-s_4)}\right\}(t)\\
&-\frac{\Gamma_N}{2\pi}\int_{-\infty}^{\infty}d\omega[1-f_N(\omega)]\mathcal{L}^{-1}\left\{\frac{s-i\varepsilon_\uparrow+\frac{\Gamma_N}{2}}{(s-s_1)(s-s_2)(s+i\omega)}\right\}(t)\mathcal{L}^{-1}\left\{\frac{1}{(s-s_3)(s-s_4)(s-i\omega)}\right\}(t)\\
&+\frac{\Gamma_N}{2\pi}\int_{-\infty}^{\infty}d\omega f_N(\omega)\mathcal{L}^{-1}\left\{\frac{1}{(s-s_1)(s-s_2)(s-i\omega)}\right\}(t)\mathcal{L}^{-1}\left\{\frac{s-i\varepsilon_\downarrow+\frac{\Gamma_N}{2}}{(s-s_3)(s-s_4)(s+i\omega)}\right\}(t)\Bigg].\end{aligned} \tag{A21}$$

4. Transient current from superconducting lead

In analogy to Eq. (15), we can define the transient current flowing from the superconductor to the quantum dot

$$j_{S\sigma}(t) = 2\mathrm{Im}\sum_{\mathbf{q}}V_{\mathbf{q}}\langle\mathcal{L}^{-1}\{\hat{d}^\dagger_\sigma(s)\}(t)\mathcal{L}^{-1}\{\hat{c}_{\mathbf{q}\sigma}(s)\}(t)\rangle. \tag{A22}$$

Laplace transforms of $\hat{d}^\dagger_\sigma(s)$ and $\hat{c}_{\mathbf{q}\sigma}(s)$ are given in Eqs. (A8) and (A10), so we can repeat the calculations similar to the ones discussed in preceding subsections. Let us consider the term proportional to $n_\uparrow(0)$, which takes the form

$$\begin{aligned}&2n_\uparrow(0)\mathrm{Im}\Bigg\{-i\sum_{\mathbf{q}}V_{\mathbf{q}}\mathcal{L}^{-1}\left\{\frac{s+i\varepsilon_\downarrow+\frac{\Gamma_N}{2}}{(s-s_1)(s-s_2)}\right\}(t)\\
&\times\left[\mathcal{L}^{-1}\left\{\frac{V_{\mathbf{q}}(s-i\varepsilon_q)\left(s-i\varepsilon_\downarrow+\frac{\Gamma_N}{2}\right)}{(s-s_3)(s-s_4)\left(s^2+\varepsilon_{\mathbf{q}}^2+\Delta^2\right)}\right\}(t)+\frac{\Gamma_S}{2}\mathcal{L}^{-1}\left\{\frac{V_{\mathbf{q}}\Delta}{(s-s_3)(s-s_4)\left(s^2+\varepsilon_{\mathbf{q}}^2+\Delta^2\right)}\right\}(t)\right]\Bigg\}.\end{aligned} \tag{A23}$$

For $\Delta = \infty$, the first term in the bottom part of this equation vanishes and we can calculate the second term by interchanging summation over $\mathbf{q}$ with the Laplace transformation:

$$2n_\uparrow(0)\mathrm{Im}\left[-i\frac{\Gamma_S}{2}\mathcal{L}^{-1}\left\{\frac{s+i\varepsilon_\downarrow+\frac{\Gamma_N}{2}}{(s-s_1)(s-s_2)}\right\}(t)\mathcal{L}^{-1}\left\{\frac{1}{(s-s_3)(s-s_4)}\sum_{\mathbf{q}}\frac{V_{\mathbf{q}}^2\Delta}{\left(s^2+\varepsilon_{\mathbf{q}}^2+\Delta^2\right)}\right\}(t)\right]. \tag{A24}$$

Since $\lim_{\Delta=\infty}\sum_{\mathbf{q}}\frac{V_{\mathbf{q}}^2\Delta}{(s^2+\varepsilon_{\mathbf{q}}^2+\Delta^2)}=\frac{\Gamma_S}{2}$ the term proportional to $n_\uparrow(0)$ simplifies to

$$2n_\uparrow(0)\frac{\Gamma_S^2}{4}\mathrm{Im}\left[-i\mathcal{L}^{-1}\left\{\frac{s+i\varepsilon_\downarrow+\frac{\Gamma_N}{2}}{(s-s_1)(s-s_2)}\right\}(t)\mathcal{L}^{-1}\left\{\frac{1}{(s-s_3)(s-s_4)}\right\}(t)\right]. \tag{A25}$$

In the same manner, we calculate the terms proportional to $\langle\hat{d}_\uparrow(0)\hat{d}_\uparrow^\dagger(0)\rangle$, $\langle\hat{c}_{\mathbf{k}\uparrow}^\dagger(0)\hat{c}_{\mathbf{k}'\uparrow}(0)\rangle$, and $\langle\hat{c}_{\mathbf{k}\uparrow}(0)\hat{c}_{\mathbf{k}'\uparrow}^\dagger(0)\rangle$, respectively. Any other terms containing expectation values of two superconducting lead electron operators vanish in the limit $\Delta=\infty$. Finally, we get the transient current

$$\begin{aligned}j_{S\sigma}(t)=\frac{\Gamma_S^2}{2}\mathrm{Re}\Bigg[&-n_\sigma(0)\,\mathcal{L}^{-1}\left\{\frac{s+i\varepsilon_{-\sigma}+\frac{\Gamma_N}{2}}{(s-s_1)(s-s_2)}\right\}(t)\mathcal{L}^{-1}\left\{\frac{1}{(s-s_3)(s-s_4)}\right\}(t)\\&+(1-n_{-\sigma}(0))\,\mathcal{L}^{-1}\left\{\frac{1}{(s-s_1)(s-s_2)}\right\}(t)\mathcal{L}^{-1}\left\{\frac{s+i\varepsilon_\sigma+\frac{\Gamma_N}{2}}{(s-s_3)(s-s_4)}\right\}(t)+\frac{\Gamma_N}{2\pi}\Phi_\sigma\Bigg],\end{aligned} \tag{A26}$$

with Φ_σ defined in Eq. (14). For $\sigma=\downarrow$, one should use the replacement $(s_1,s_2,s_3,s_4)\to(s_3,s_4,s_1,s_2)$. In theequilibrium case (for $\mu_N=0$), the formula Eq. (A26) can be simplified, because $\mathrm{Re}\Phi_\sigma=0$. To prove this property, let us focus on the case $\varepsilon_\sigma=0$, when we can express $\Phi_\sigma=\sum_{j=1}^4\int_{-\infty}^{\infty}d\varepsilon(1-2f_N(\varepsilon))A_j(\varepsilon)$ using the coefficients

$$\begin{aligned}A_1(\varepsilon)&=\frac{-ie^{-\Gamma_N t}}{2\Gamma_S}\left[\frac{e^{i\Gamma_S t}}{\left(\frac{\Gamma_N}{2}-i\varepsilon_+\right)\left(\frac{\Gamma_N}{2}+i\varepsilon_-\right)}-\frac{e^{-i\Gamma_S t}}{\left(\frac{\Gamma_N}{2}-i\varepsilon_-\right)\left(\frac{\Gamma_N}{2}+i\varepsilon_+\right)}\right],\\A_2(\varepsilon)&=\frac{ie^{-\Gamma_N t}\varepsilon}{\left(\frac{\Gamma_N^2}{4}+\varepsilon_+^2\right)\left(\frac{\Gamma_N^2}{4}+\varepsilon_-^2\right)},\\A_3(\varepsilon)&=-\frac{\frac{\Gamma_N}{2}+i\varepsilon}{\left(\frac{\Gamma_N^2}{4}+\varepsilon_-^2\right)\left(\frac{\Gamma_N^2}{4}+\varepsilon_+^2\right)},\\A_4(\varepsilon)&=-\frac{e^{-\Gamma_N t/2}}{2}\left[\frac{e^{-i\varepsilon_+ t}}{\left(\frac{\Gamma_N^2}{4}+\varepsilon_+^2\right)\left(\frac{\Gamma_N}{2}-i\varepsilon_-\right)}+\frac{e^{-i\varepsilon_- t}}{\left(\frac{\Gamma_N^2}{4}+\varepsilon_-^2\right)\left(\frac{\Gamma_N}{2}-i\varepsilon_+\right)}\right]\\&\quad-\frac{ie^{-\Gamma_N t/2}}{\Gamma_S}\left(\frac{\Gamma_N}{2}+i\varepsilon\right)\left[\frac{-e^{i\varepsilon_+ t}}{\left(\frac{\Gamma_N^2}{4}+\varepsilon_+^2\right)\left(\frac{\Gamma_N}{2}+i\varepsilon_-\right)}+\frac{e^{i\varepsilon_- t}}{\left(\frac{\Gamma_N^2}{4}+\varepsilon_-^2\right)\left(\frac{\Gamma_N}{2}+i\varepsilon_+\right)}\right],\end{aligned} \tag{A27}$$

and $\varepsilon_{+/-}=\varepsilon\pm\frac{\Gamma_S}{2}$. At zero temperature, this function can be given as $\Phi_\sigma=\sum_{j=1}^4\int_0^\infty d\varepsilon(A_j(\varepsilon)-A_j(-\varepsilon))$, using the following properties: $A_1(\varepsilon)=A_1(-\varepsilon)$, $A_2(\varepsilon)=-A_2(-\varepsilon)$, $\mathrm{Re}A_3(\varepsilon)=\mathrm{Re}A_3(-\varepsilon)$ and $A_4(-\varepsilon)=A_4^*(\varepsilon)$, which imply that $\mathrm{Re}\Phi_\sigma=0$. The same conclusion is valid for $\varepsilon_\sigma\neq0$ as well.

APPENDIX B: MEAN FIELD APPROXIMATION

In this brief Appendix, we consider the effective Hamiltonian of the proximitized QD coupled to the normal lead, treating electron correlations within the Hartree-Fock-Bogoliubov approximation:

$$\hat{H}=\sum_\sigma(\varepsilon_\sigma+Un_{-\sigma}(t))\hat{d}_\sigma^\dagger\hat{d}_\sigma+\left[\left(\frac{\Gamma_S}{2}+U\chi(t)\right)\hat{d}_\uparrow^\dagger\hat{d}_\downarrow^\dagger+\mathrm{H.c.}\right]+\sum_{\mathbf{k},\sigma}[V_{\mathbf{k}}\hat{d}_\sigma^\dagger\hat{c}_{\mathbf{k}\sigma}+\mathrm{H.c.}]+\sum_{\mathbf{k},\sigma}\varepsilon_{\mathbf{k}\sigma}\hat{c}_{\mathbf{k}\sigma}^\dagger\hat{c}_{\mathbf{k}\sigma}. \tag{B1}$$

In general, all parameters ε_σ, Γ_S, $V_{\mathbf{k}}$, $\varepsilon_{\mathbf{k}\sigma}$ can be time-dependent. In what follows, we outline the algorithm for numerical computation of the QD charge $n_\sigma(t)$ and the induced on-dot pairing $\chi(t)=\langle\hat{d}_\downarrow(t)\hat{d}_\uparrow(t)\rangle$. We have to solve numerically the following set of coupled equations of motion:

$$\frac{dn_\sigma(t)}{dt}=2\mathrm{Im}\left(\sum_{\mathbf{k}}V_{\mathbf{k}}e^{i\varepsilon_{\mathbf{k}}t}\langle\hat{d}_\sigma^\dagger(t)\hat{c}_{\mathbf{k}\sigma}(0)\rangle-\bar{\Delta}^*(t)\chi(t)-\Gamma_N n_\sigma(t)\right), \tag{B2}$$

$$\frac{d\chi(t)}{dt}=i\sum_{\mathbf{k}}V_{\mathbf{k}}e^{-i\varepsilon_{\mathbf{k}}t}(\langle\hat{d}_\uparrow(t)\hat{c}_{\mathbf{k}\downarrow}(0)\rangle-\langle\hat{d}_\downarrow(t)\hat{c}_{\mathbf{k}\uparrow}(0)\rangle)-[i(\bar{\varepsilon}_\uparrow(t)+\bar{\varepsilon}_\downarrow(t))+\Gamma_N]\chi(t)-i\bar{\Delta}(t)(1-n_\downarrow(t)-n_\uparrow(t)), \tag{B3}$$

where $\bar{\varepsilon}_\sigma(t) = \varepsilon_\sigma + Un_{-\sigma}(t)$ and $\bar{\Delta}(t) = \frac{\Gamma_S}{2} + U\chi(t)$. In the wide-band-limit approximation and assuming $\varepsilon_{\mathbf{k}\sigma}$ to be time-independent, the mixed functions appearing in Eqs. (B2) and (B3) can be determined from the equations of motion:

$$\frac{d}{dt}\langle \hat{d}^\dagger_\sigma(t)\hat{c}_{\mathbf{k}\sigma}(0)\rangle = \left(i\bar{\varepsilon}_\sigma(t) - \frac{\Gamma_N}{2}\right)\langle \hat{d}^\dagger_\sigma(t)\hat{c}_{\mathbf{k}\sigma}(0)\rangle + i\alpha\bar{\Delta}^*(t)\langle \hat{d}_{-\sigma}(t)\hat{c}_{\mathbf{k}\sigma}(0)\rangle + iV_{\mathbf{k}}e^{i\varepsilon_{\mathbf{k}}t}f_N(\varepsilon_{\mathbf{k}}), \tag{B4}$$

$$\frac{d}{dt}\langle \hat{d}_\sigma(t)\hat{c}_{\mathbf{k}-\sigma}(0)\rangle = -\left(i\bar{\varepsilon}_\sigma(t) + \frac{\Gamma_N}{2}\right)\langle \hat{d}_\sigma(t)\hat{c}_{\mathbf{k}-\sigma}(0)\rangle - i\alpha\bar{\Delta}(t)\langle \hat{d}^\dagger_\sigma(t)\hat{c}_{\mathbf{k}\sigma}(0)\rangle, \tag{B5}$$

where $\alpha = +(-)$ for $\sigma = \uparrow(\downarrow)$ and $f_N(\varepsilon_{\mathbf{k}})$ is the Fermi-Dirac distribution of mobile electrons in the normal lead.

[1] A. V. Balatsky, I. Vekhter, and J.-X. Zhu, Impurity-induced states in conventional and unconventional superconductors, Rev. Mod. Phys. **78**, 373 (2006).

[2] A. Martín-Rodero and A. Levy Yeyati, Josephson and Andreev transport through quantum dots, Adv. Phys. **60**, 899 (2011).

[3] A. Yazdani, B. A. Jones, C. P. Lutz, M. F. Crommie, and D. M. Eigler, Probing the local effects of magnetic impurities on superconductivity, Science **275**, 1767 (1997).

[4] B. W. Heinrich, J. I. Pascual, and K. J Franke, Single magnetic adsorbates on s-wave superconductors, Prog. Surf. Sci. **93**, 1 (2018).

[5] S. De Franceschi, L. Kouwenhoven, C. Schönenberger, and W. Wernsdorfer, Hybrid superconductor-quantum dot devices, Nat. Nanotechnol. **5**, 703 (2010).

[6] R. S. Deacon, Y. Tanaka, A. Oiwa, R. Sakano, K. Yoshida, K. Shibata, K. Hirakawa, and S. Tarucha, Kondo-enhanced Andreev transport in single self-assembled InAs quantum dots contacted with normal and superconducting leads, Phys. Rev. B **81**, 121308 (2010).

[7] J. Schindele, A. Baumgartner, R. Maurand, M. Weiss, and C. Schönenberger, Nonlocal spectroscopy of Andreev bound states, Phys. Rev. B **89**, 045422 (2014).

[8] J. Gramich, A. Baumgartner, and C. Schönenberger, Andreev bound states probed in three-terminal quantum dots, Phys. Rev. B **96**, 195418 (2017).

[9] R. Seoane Souto, A. Martín-Rodero, and A. Levy Yeyati, Quench dynamics in superconducting nanojunctions: Metastability and dynamical Yang-Lee zeros, Phys. Rev. B **96**, 165444 (2017).

[10] J. Eisert, M. Friesdorf, and C. Gogolin, Quantum many-body systems out of equilibrium, Nat. Phys. **11**, 124 (2015).

[11] K. Bidzhiev and G. Misguich, Out-of-equilibrium dynamics in a quantum impurity model: Numerics for particle transport and entanglement entropy, Phys. Rev. B **96**, 195117 (2017).

[12] Q.-F. Sun, B.-G. Wang, J. Wang, and T.-H. Lin, Electron transport through a mesoscopic hybrid multiterminal resonant-tunneling system, Phys. Rev. B **61**, 4754 (2000).

[13] H.-K. Zhao and J. Wang, Zeeman-split mesoscopic transport through a normal-metal–quantum-dot–superconductor system with ac response, Phys. Rev. B **64**, 094505 (2001).

[14] Y. Wei and J. Wang, Carbon-nanotube-based quantum pump in the presence of a superconducting lead, Phys. Rev. B **66**, 195419 (2002).

[15] Z. Cao, T.-F. Fang, L. Li, and H.-G. Luo, Thermoelectric-induced unitary Cooper pair splitting efficiency, Appl. Phys. Lett. **107**, 212601 (2015).

[16] G. Stefanucci and C. O. Almbladh, Time-dependent partition-free approach in resonant tunneling systems, Phys. Rev. B **69**, 195318 (2004).

[17] J. Maciejko, J. Wang, and H. Guo, Time-dependent quantum transport far from equilibrium: An exact nonlinear response theory, Phys. Rev. B **74**, 085324 (2006).

[18] F. M. Souza, S. A. Leão, R. M. Gester, and A. P. Jauho, Transient charging and discharging of spin-polarized electrons in a quantum dot, Phys. Rev. B **76**, 125318 (2007).

[19] T. L. Schmidt, P. Werner, L. Muhlbacher, and A. Komnik, Transient dynamics of the Anderson impurity model out of equilibrium, Phys. Rev. B **78**, 235110 (2009).

[20] A. Komnik, Transient dynamics of the nonequilibrium Majorana resonant level model, Phys. Rev. B **79**, 245102 (2009).

[21] Ph. Werner, T. Oka, M. Eckstein, and A. J. Millis, Weak-coupling quantum Monte Carlo calculations on the Keldysh contour: Theory and application to the current-voltage characteristics of the Anderson model, Phys. Rev. B **81**, 035108 (2010).

[22] J. Jin, Matisse Wei-Yuan Tu, W.-M. Zhang, and YiJing Yan, Non-equilibrium quantum theory for nanodevices based on the Feynman Vernon influence functional, New J. Phys. **12**, 083013 (2010).

[23] D. Segal, A. Millis, and D. Reichman, Nonequilibrium transport in quantum impurity models: exact path integral simulations, Phys. Chem. Chem. Phys. **13**, 14378 (2011).

[24] K. Joho, S. Maier, and A. Komnik, Transient noise spectra in resonant tunneling setups: Exactly solvable models, Phys. Rev. B **86**, 155304 (2012).

[25] M. Kulkarni, K. Tiwari, and D. Segal, Full density matrix dynamics for large quantum systems: interactions, decoherence and inelastic effects, New J. Phys. **15**, 013014 (2013).

[26] K. F. Albrecht, A. Martin-Rodero, R. C. Monreal, L. Mühlbacher, and A. Levy Yeyati, Long transient dynamics in the Anderson-Holstein model out of equilibrium, Phys. Rev. B **87**, 085127 (2013).

[27] R. Tuovinen, E. Perfetto, G. Stefanucci, and R. van Leeuwen, Time-dependent Landauer-Büttiker formula: Application to transient dynamics in graphene nanoribbons, Phys. Rev. B **89**, 085131 (2014).

[28] M. M. Odashima and C. H. Lewenkopf, Time-dependent resonant tunneling transport: Keldysh and Kadanoff-Baym nonequilibrium Green's functions in an analytically soluble problem, Phys. Rev. B **95**, 104301 (2017).

[29] S.-H. Ke, R. Liu, W. Yang, and H. U. Baranger, Time-dependent transport through molecular junctions, J. Chem. Phys. **132**, 234105 (2010).

[30] K. Yamada, T. Yamamoto, and K. Watanabe, Transient current behavior of nanoscale objects: Role of displacement current and polaron effects, Jpn. J. Appl. Phys. **48**, 075001 (2009).

[31] X. Chen, J. Yuan, G. Tang, J. Wang, Z. Zhang, C.-M. Hu, and H. Guo, Transient spin current under a thermal switch, J. Phys. D: Appl. Phys. **51**, 274004 (2018).

[32] V. Vovchenko, D. Anchishkin, J. Azema, P. Lombardo, R. Hayn, and A.-M. Daré, A new approach to time-dependent transport through an interacting quantum dot within the Keldysh formalism, J. Phys.: Condens. Matter **26**, 015306 (2014).

[33] J. Orenstein, Ultrafast spectroscopy of quantum materials, Phys. Today **65**(9), 44 (2012).

[34] C. L. Smallwood, R. A. Kaindl, and A. Lanzara, Ultrafast angle-resolved photoemission spectroscopy of quantum materials, Europhys. Lett. **115**, 27001 (2016).

[35] P. Nordlander, M. Pustilnik, Y. Meir, N. S. Wingreen, and D. C. Langreth, How Long Does It Take for the Kondo Effect to Develop? Phys. Rev. Lett. **83**, 808 (1999).

[36] G. Michałek and B. R. Bułka, Dynamical correlations in electronic transport through a system of coupled quantum dots, Phys. Rev. B **80**, 035320 (2009).

[37] R. Seoane Souto, R. Avriller, R. C. Monreal, A. Martín-Rodero, and A. Levy Yeyati, Transient dynamics and waiting time distribution of molecular junctions in the polaronic regime, Phys. Rev. B **92**, 125435 (2015).

[38] Q.-F. Sun, J. Wang, and T.-H. Lin, Photon-assisted Andreev tunneling through a mesoscopic hybrid system, Phys. Rev. B **59**, 13126 (1999).

[39] Y. Xing, Q.-F. Sun, and J. Wang, Response time of a normal-metal/superconductor hybrid system under a steplike pulse bias, Phys. Rev. B **75**, 125308 (2007).

[40] G. Stefanucci, E. Perfetto, and M. Cini, Time-dependent quantum transport with superconducting leads: A discrete-basis Kohn-Sham formulation and propagation scheme, Phys. Rev. B **81**, 115446 (2010).

[41] L. D. Contreras-Pulido, J. Splettstoesser, M. Governale, J. König, and M. Büttiker, Time scales in the dynamics of an interacting quantum dot, Phys. Rev. B **85**, 075301 (2012).

[42] K. F. Albrecht, H. Soller, L. Muhlbacher, and A. Komnik, Transient dynamics and steady state behavior of the Anderson-Holstein model with a superconducting lead, Physica E (Amsterdam) **54**, 15 (2013).

[43] K. J. Pototzky and E. K. U. Gross, Controlling observables in time-dependent quantum transport, arXiv:1407.2554.

[44] L. Rajabi, C. Pöltl, and M. Governale, Waiting Time Distributions for the Transport Through a Quantum-Dot Tunnel Coupled to One Normal and One Superconducting Lead, Phys. Rev. Lett. **111**, 067002 (2013).

[45] G. Michałek, B. R. Bułka, T. Domański, and K. I. Wysokiński, Statistics of tunneling events in three-terminal hybrid devices with quantum dot, Acta Phys. Pol. A **133**, 391 (2018).

[46] S. Mi, P. Burset, and Ch. Flindt, Electron waiting times in hybrid junctions with topological superconductors, arXiv:1805.01704.

[47] N. Walldorf, C. Padurariu, A.-P. Jauho, and Ch. Flindt, Electron Waiting Times of a Cooper Pair Splitter, Phys. Rev. Lett. **120**, 087701 (2018).

[48] P. Stegmann and J. König, Short-time counting statistics of charge transfer in Coulomb-blockade systems, Phys. Rev. B **94**, 125433 (2016).

[49] H. Soller and A. Komnik, Full counting statistics of interacting quantum dots contacted by a normal metal and a superconductor, Europhys. Lett. **106**, 37009 (2014).

[50] V. F. Maisi, D. Kambly, Ch. Flindt, and J. P. Pekola, Full Counting Statistics of Andreev Tunneling, Phys. Rev. Lett. **112**, 036801 (2014).

[51] R. Seoane Souto, A. Martín-Rodero, and A. Levy Yeyati, Andreev Bound States Formation and Quasiparticle Trapping in Quench Dynamics Revealed by Time-Dependent Counting Statistics, Phys. Rev. Lett. **117**, 267701 (2016).

[52] S. Droste, J. Splettstoesser, and M. Governale, Finite-frequency noise in a quantum dot with normal and superconducting leads, Phys. Rev. B **91**, 125401 (2015).

[53] D. Futterer, J. Swiebodzinski, M. Governale, and J. König, Renormalization effects in interacting quantum dots coupled to superconducting leads, Phys. Rev. B **87**, 014509 (2013).

[54] J. Eldridge, M. G. Pala, M. Governale, and J. König, Superconducting proximity effect in interacting double-dot systems, Phys. Rev. B **82**, 184507 (2010).

[55] V. Janiš, Wiener-Hopf method applied to the x-ray edge problem, Int. J. Mod. Phys. B **11**, 3433 (1997).

[56] P. Nozierés and C. De Dominicis, Singularities in the x-ray absorption and emission of metals. III. One-body theory exact solution, Phys. Rev. **178**, 1097 (1969).

[57] R. S. Deacon, Y. Tanaka, A. Oiwa, R. Sakano, K. Yoshida, K. Shibata, K. Hirakawa, and S. Tarucha, Tunneling Spectroscopy of Andreev Energy Levels in a Quantum Dot Coupled to a Superconductor, Phys. Rev. Lett. **104**, 076805 (2010).

[58] J.-D. Pillet, P. Joyez, R. Žitko, and M. F. Goffman, Tunneling spectroscopy of a single quantum dot coupled to a superconductor: From Kondo ridge to Andreev bound states, Phys. Rev. B **88**, 045101 (2013).

[59] A. Eichler, M. Weiss, S. Oberholzer, C. Schönenberger, A. Levy Yeyati, J. C. Cuevas, and A. Martín-Rodero, Even-Odd Effect in Andreev Transport through a Carbon Nanotube Quantum Dot, Phys. Rev. Lett. **99**, 126602 (2007).

[60] C. Cohen-Tannoudji, B. Diu, and F. Laloe, *Quantum Mechanics*, Vol. 1 (Wiley-Interscience Publications, Paris, 1977).

[61] A.-P. Jauho, N. S. Wingreen, and Y. Meir, Time-dependent transport in interacting and noninteracting resonant-tunneling systems, Phys. Rev. B **50**, 5528 (1994).

[62] M. Žonda, V. Pokorný, V. Janiš, and T. Novotný, Perturbation theory of a superconducting 0 - π impurity quantum phase transition, Sci. Rep. **5**, 8821 (2015).

[63] T. Domański and A. Donabidowicz, Interplay between particle-hole splitting and the Kondo effect in quantum dots, Phys. Rev. B **78**, 073105 (2008).

[64] J. Bauer, A. Oguri, and A. C. Hewson, Spectral properties of locally correlated electrons in a Bardeen-Cooper-Schrieffer superconductor, J. Phys.: Condens. Matter **19**, 486211 (2007).

[65] E. J. H. Lee, X. Jiang, R. Aguado, G. Katsaros, C. M. Lieber, and S. De Franceschi, Zero-Bias Anomaly in a Nanowire Quantum Dot Coupled to Superconductors, Phys. Rev. Lett. **109**, 186802 (2012).

[66] R. Žitko, J. S. Lim, R. López, and R. Aguado, Shiba states and zero-bias anomalies in the hybrid normal-superconductor Anderson model, Phys. Rev. B **91**, 045441 (2015).

[67] T. Domański, I. Weymann, M. Barańska, and G. Górski, Constructive influence of the induced electron pairing on the Kondo state, Sci. Rep. **6**, 23336 (2016).

[68] T. Domański, M. Žonda, V. Pokorný, G. Górski, V. Janiš, and T. Novotný, Josephson-phase-controlled interplay between correlation effects and electron pairing in a three-terminal nanostructure, Phys. Rev. B **95**, 045104 (2017).

[69] C. Janvier, L. Tosi, L. Bretheau, Ç. Ö. Girit, M. Stern, P. Bertet, P. Joyez, D. Vion, D. Esteve, M. F. Goffman, H. Pothier, and C. Urbina, Coherent manipulation of Andreev states in superconducting atomic contacts, Science **349**, 1199 (2015).